Nano Research 2017, 10(5): 1560–1583
DOI 10.1007/s12274-017-1476-8
Review Article
ISSN 1998-0124
CN 11-5974/O4

Recent progress in flexible and wearable bio-electronics based on nanomaterials

Yanbing Yang, Xiangdong Yang, Yaning Tan, and Quan Yuan (✉)

Key Laboratory of Analytical Chemistry for Biology and Medicine (Ministry of Education), College of Chemistry and Molecular Sciences, Wuhan University, Wuhan 430072, China

Received: 29 September 2016
Revised: 2 January 2017
Accepted: 5 January 2017

KEYWORDS
flexible biosensor, electronics, nanostructured materials, integrated devices, graphene

ABSTRACT

Flexible and stretchable biosensors that can monitor and quantify the electrical or chemical signals generated by specific microenvironments have attracted a great deal of attention. Wearable biosensors that can be intimately attached to skin or tissue provide a new opportunity for medical diagnostics and therapy. In recent years, there has been enormous progress in device integration and the design of materials and manufacturing processes for flexible and stretchable systems. Here, we describe the most recent developments in nanomaterials employed in flexible and stretchable biosensors. We review successful examples of such biosensors used for the detection of vital physiological and biological markers such as gas released from organisms. Furthermore, we provide a detailed overview of recent achievements regarding integrated platforms that include multifunctional nanomaterials. The issues and challenges related to the effective integration of multifunctional nanomaterials in bio-electronics are also discussed.

1 Introduction

Flexible electronics may be incorporated into wearable devices that can accommodate dramatic mechanical deformations while maintaining stable performance [1–4]. Recently, flexible biosensors have attracted the attention of researchers owing to their potential usefulness in personal healthcare and disease diagnosis [5–8]. Flexible and wearable biosensors have several intriguing advantages; they are light-weight, ultra-conformable, portable, noninvasive, and implantable. They can be attached to the tissue surface and can continuously and closely monitor physiological biomarkers and the electronic, electrochemical, thermal, mechanical, and biochemical signals emanating from the human body without interrupting or influencing an individual's activities [9–11]. Therefore, the development of inexpensive, wearable systems for the rapid *in situ* detection and measurement of vital signals in the human body provides an opportunity for designing point-of-care clinical devices for disease diagnosis, therapy, and health monitoring.

Typically, flexible biosensors are composed of several essential parts: 1) a flexible substrate that supports the

Address correspondence to yuanquan@whu.edu.cn

entire circuit and simultaneously conforms to irregular structures [12–14]; 2) electrodes or active materials for electronic or optical signal export [15–17]; and 3) specific sensing elements for recognizing analytes [18–21]. The development of flexible and stretchable biosensors requires a novel approach to material design regarding the selection of suitable nanomaterials and the synthesis of new multifunctional nanomaterials [22–24]. New sensing materials, fabrication techniques, and sensing mechanisms have significantly promoted the development of flexible and stretchable biosensors [25–27]. Recently, research interest has focused on multiple sensors that are integrated into a single sensor network [28]. Such sensor systems are required to simultaneously measure multiple stimuli because the human body can generate physical information as well as chemical and biological signals under stimulation. Therefore, integrated systems with physical and chemical or biological sensors are of vital importance for the development of advanced flexible biosensors with multiple functions [29]. The integration of biosensors with medical treatment and data processing systems is another requirement of wearable sensors [30, 31]. More recently, a few research groups have demonstrated integrated systems that combine pH and glucose sensors with drug delivery systems for diabetes diagnosis and therapy [32].

Here, we summarize the recent progress made in the development of flexible and stretchable biosensors that can be used as wearable devices, with regard to the various nanomaterials, nanostructures, and engineering technologies used. We provide a brief introduction to the general working principle of biosensors based on different types of components used to monitor vital signals such as those pertaining to heart and respiration rate, diabetes, DNA, and cancer biomarkers. We also summarize detailed descriptions of the development of flexible biosensors in conjunction with device design. In particular, we provide an overview of flexible biosensors with integrated systems together with examples of flexible biosensors reported in the literature. The issues and challenges faced by flexible biosensors are comprehensively discussed. Overall, in this review, we present the recent advances in nanomaterials used in flexible biosensors. We also provide an overview of the recent progress made in the development of flexible bioelectronics based on integrated device designs. The challenges and future opportunities presented by flexible biosensors based on nanomaterials are also discussed.

2 Materials for flexible biosensors

The flexible substrate plays an important role in device development because it acts as a mechanical support for active materials and electronic circuits. Apart from flexibility, the substrate should be bendable, stretchable, transparent, and even biodegradable. Polyethylene terephthalate (PET) and polyimide (PI) are the most widely used substrates in flexible biosensor fabrication owing to their high thermal and chemical resistance [33–36]. In addition to flexibility, the remarkable elasticity of polydimethylsiloxane (PDMS) makes it the best choice for stretchable sensors [37, 38]. Natural biomaterials such as silk are considered excellent candidates for implantable biosensors owing to their excellent characteristics such as biocompatibility, biodegradability, and natural abundance [39, 40]. Large area patterned conducting polymers such as polypyrrole (PPy), polyaniline (PANI), and polythiophene can also be used as the active materials in biosensors [41–43]. The polythiophene derivative poly(3,4-ethylenedioxythiophene):poly(styrene sulfonate) (PEDOT:PSS) is the most commonly used organic semiconductor for chemical and biological sensing applications [44].

Recently, nanomaterials have been explored in the context of flexible biosensor applications because they provide tunable nanostructures. Figure 1 shows representative nanomaterials used in flexible and stretchable devices. Nanomaterials can be patterned to form films or arrays to provide mechanical flexibility, thereby resolving the intrinsic mechanical mismatch between rigid devices and curvilinear biological structures. Furthermore, the nanoscale dimensions of nanostructured materials endow them with large surface areas that significantly increase the effective contact area, which is an advantage for flexible biosensors that require high sensitivity. The development of nanomaterials with favorable electrical and mechanical properties facilitates the fabrication of

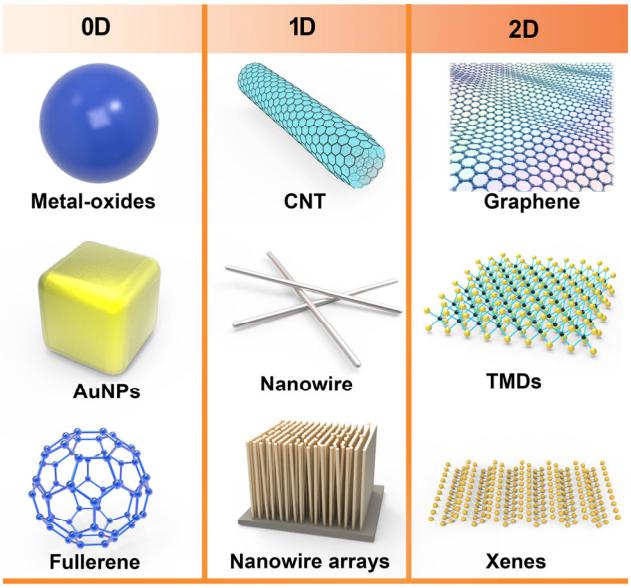

Figure 1 Representative nanomaterials used for flexible and stretchable devices.

wearable and flexible biosensors. Here, we provide a comprehensive review of nanomaterials with different dimensions (0D, 1D, 2D, and composites) for flexible and stretchable devices.

2.1 0D-nanoparticles

Owing to the advantages of large-scale production and fast film deposition over large areas, metal oxide-based semiconductors have been widely used in various applications such as sensors [45], field-effect transistors (FETs) [46], and energy storage and conversion [47]. FET-based biosensors in particular have emerged as one of the most attractive bio-electronic options because they facilitate rapid electronic detection, are label-free, consume little power, and allow the integration of sensors and measurement systems [44, 48]. When they are integrated with flexible substrates, metal oxides can serve as highly reproducible flexible sensors owing to their large-area electronic uniformity. In addition to a flexible support, sensors based on metal oxide semiconductors also comprise two or three electrodes for electrical output, with the metal oxide material as the active channel. The conductivity of the device increases or decreases when the metal oxide encounters target analytes. TiO_2 [49], V_2O_5 [50], WO_3 [51], ZnO [52–54], SnO_2 [55], In_2O_3 [45], and Ga_2O_3 [56] are examples of commonly used metal oxide semiconductor materials. Tseng et al. [45] recently reported a conformal FET biosensor based on ultrathin PI films printed with In_2O_3 (Fig. 2). The use of an ultrathin In_2O_3 film and the flexibility of the substrate enabled highly conformal contact between the device and complex curvilinear surfaces. Once the In_2O_3-based transistor device had been functionalized with glucose oxidase, a biosensor integrated into an artificial eye was able to detect the glucose in tears with high sensitivity and selectivity. This conformal FET-based biosensor offers new opportunities for future wearable human technologies.

2.2 1D-nanowires and nanotubes

1D nanowires (NWs) and nanotubes with a large surface-to-volume ratio facilitate a significant change in conductance under a small local charge variation on the wire surface, owing to the electric field effect [58–60]. Nanowires and nanotubes can be patterned into aligned configurations or percolated networks to serve as the active component of flexible devices. Moreover, solution-processed 1D nanomaterials can also be printed to form 3D conductive networks, which can be used in freestanding flexible biosensors [26]. Silicon nanowires (SiNWs) have many favorable properties such as large on/off ratios and high charge carrier mobility, and they are easily produced on a large scale, which makes them ideal for applications in electronics, biosensors, and general technology [60, 61]. In particular, SiNW FETs are potentially useful in highly sensitive biomolecular detectors [62, 63]. The functionalization of SiNWs can be used to improve sensing selectivity and sensitivity, and to control the device dimensions and response time. Tian et al. [59] designed a hybrid architecture by inserting 3D macroporous, flexible, and free-standing SiNW FET-based nanoelectronic scaffolds (nanoES) into synthetic or natural biomaterials (Fig. 3). As with natural tissue scaffolds, hybrid nanoES structures with superior biocompatibility can be used for the 3D culture of neuron cells, cardiomyocytes, and smooth muscle cells. More importantly, the SiNW nanoES in the nanoES/cardiomyocyte constructs can be used to monitor the local electrical activity of cardiomyocytes in real time. Furthermore, the responses of the 3D nanoES-based

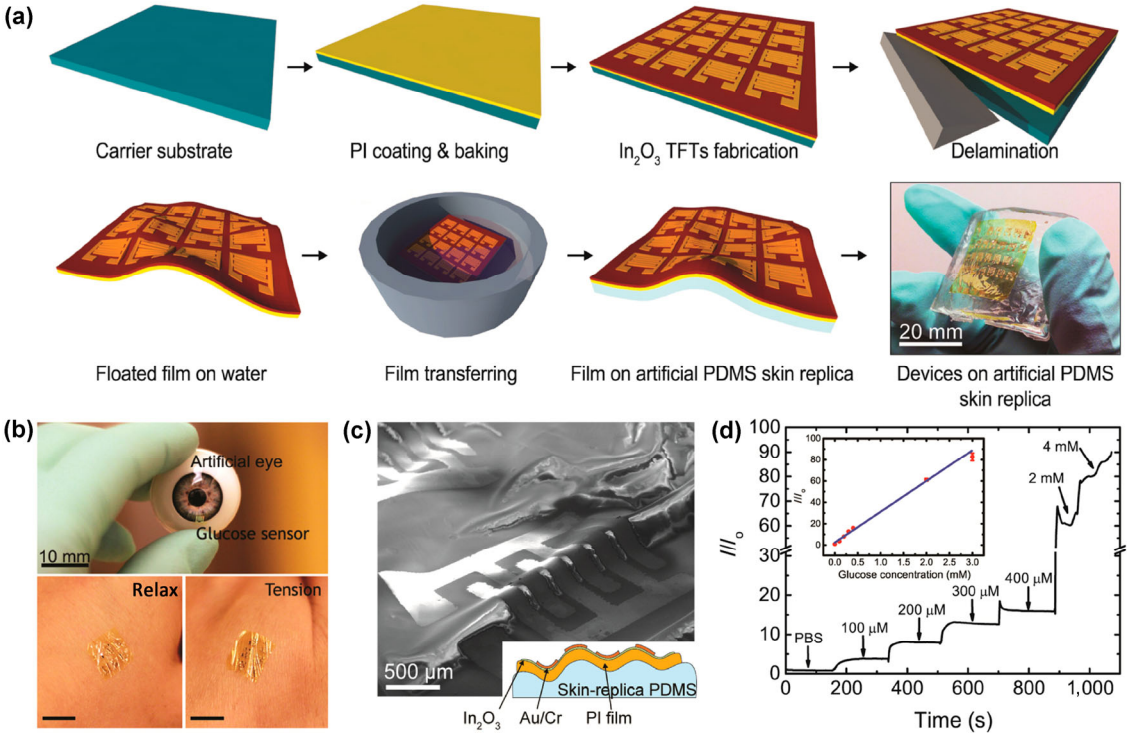

Figure 2 (a) Schematic illustration of the synthesis of the flexible biosensor. (b) Images of conformally contacted devices on an artificial eye; the thin film sensors remained in contact with the skin even during tension and relaxation. (c) Scanning electron microscope image of a representative device on an artificial PDMS skin replica. (d) Representative responses of In_2O_3 sensors to D-glucose concentrations in human diabetic tears (lower range) and blood (upper range). Inset shows data from five devices. (Reproduced with permission from Ref. [45], © American Chemical Society 2015.)

neural and cardiac tissue models to drugs and the pH variations inside and outside tubular vascular muscle constructs illustrate the superior sensing performance of SiNW FET devices.

Apart from NWs, 1D tubular structures such as carbon nanotubes (CNTs) [64] with favorable electrical properties along the axial direction have been the subject of intense scrutiny since their discovery in 1991. By controlling their synthesis conditions, CNTs can be assembled into films [65], forests [66], aerogels [67], and sponges [68–70]. Owing to the advantages of low density, high aspect ratio, and flexibility, CNTs are considered ideal candidates for flexible conductors in light-weight and wearable device arrays. Kim et al. [71] reported a hierarchically engineered, elastic CNT fabric-based multimodal sensor that is wearable and highly sensitive (Fig. 4). The CNTs are assembled into microyarns that retain the mechanical strength and electrical/thermal conductivity of individual CNTs. Devices with piezocapacitive architecture can be produced by the incorporation of CNT microyarn circuitry into stretchable dielectric PDMS (Ecoflex) substrates. The aligned CNT microyarns allow point-to-point overlap to enable the development of devices with high sensitivity and spatial resolution. In this regard, the change of resistance or capacitance resulting from mechanical deformations such as touch, or changes in temperature, humidity gradients, or even biological variables, can be detected by such multimodal-output electric devices.

2.3 2D-nanostructure

2D nanostructures are layered crystalline solids comprising atom-thin nanosheets. Such nanosheets interact with each other through van der Waals bonding. Currently developed 2D nanosheets include graphene [72–78], transition metal dichalcogenides (TMDs) [79–89], diatomic hexagonal boron nitride (h-BN) [90–92], black phosphorene [93–95], and MXenes [96–99]. MXenes are 2D transition metal carbides; "M"

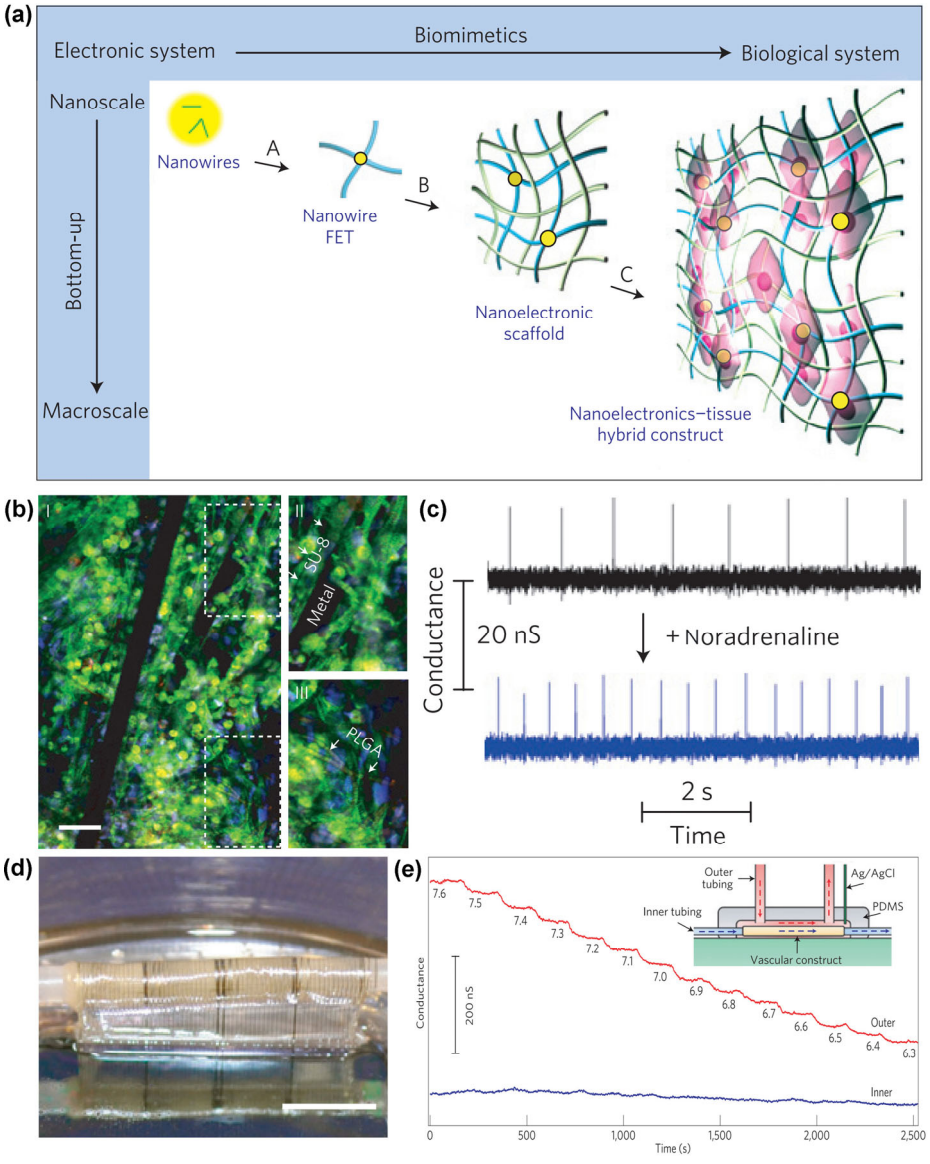

Figure 3 (a) Schematic illustration of the fabrication process of nanoES-tissue hybrid constructs. (b) Confocal fluorescence micrographs of the nanoES and poly(lactic-co-glycolic acid) (PLGA) hybrid scaffolds cultured with cardiomyocytes. (c) Electrical recording of the response of the nanoES-based hybrids toward noradrenaline stimulation. Scale bar, 40 μm. (d) Optical image of the nanoES-based vascular construct after rolling into a tube. Scale bar, 5 mm. (e) Conductance change versus time for two SiNW FET devices located in the outermost and innermost layers. Inset is a schematic of the experimental set-up. (Reproduced with permission from Ref. [59], © Nature Publishing Group 2012.)

represents a transition metal, and "X" represents carbon or nitrogen. The outstanding electrical and mechanical properties of 2D crystals have generated enormous interest in the fields of semiconductor technology and flexible nanotechnology research. To date, the most commonly used materials for constructing flexible biosensors are graphene and TMDs. We will now provide a discussion of biosensors based on these two nanostructured 2D materials.

2.3.1 *Graphene*

Since its discovery in 2004, graphene has attracted considerable attention owing to its remarkable electrical, optical, mechanical, thermal, and biocompatibility properties [100–103]. Graphene has outstanding physical properties including high carrier mobility and capacity,

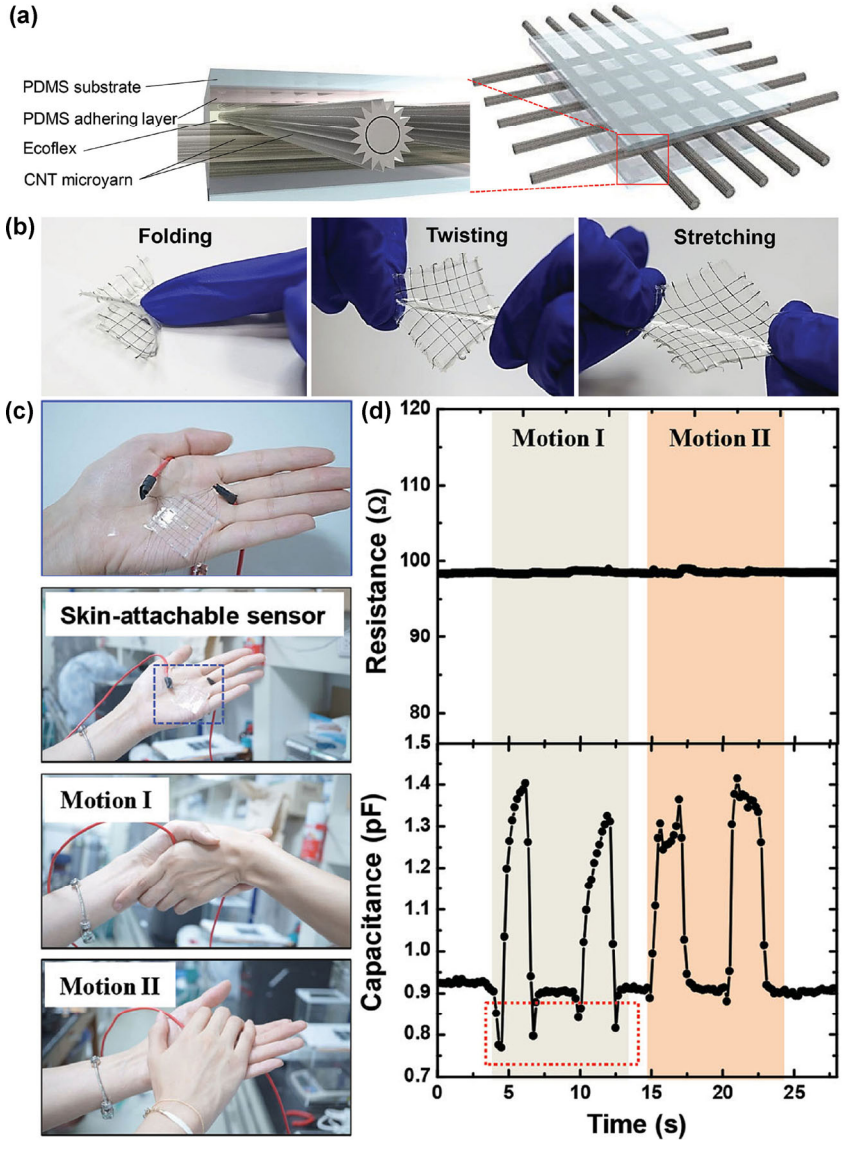

Figure 4 (a) Schematic view of the active layers of CNT microyarn-based sensor skin. (b) Photographs of the all-carbon-based device under folding, twisting, and stretching deformations. (c) Photographs of the skin-attachable sensor incorporated onto the palm with different motions. (d) Resistance and capacitance variation of the CNT microyarn under motions. (Reproduced with permission from Ref. [71], © John Wiley & Sons 2015.)

an ultrathin form factor, an ambipolar field effect, and highly tunable conductance; it is therefore very useful in science and technology [104–106]. Graphene comprises a 2D, single atom-thick honeycomb lattice of carbon atoms; it has exceptional mechanical strength and flexibility, which makes it very useful for flexible electronic devices [105, 107, 108]. The properties of graphene can be tuned by chemical doping or functionalization with receptor molecules, and it is therefore suitable for high-performance flexible nanoelectronic sensors.

The combination of a PET substrate and graphene materials facilitates the development of flexible graphene-based biosensors. Flexible graphene-based biosensors have been used to detect a variety of biological indicators including DNA, proteins, organic molecules, cells, the gas released from bio-systems, and pH levels [109–113]. Reduced graphene oxide (RGO)-based biosensors have the advantages of device structure simplicity and label-free detection [20, 114].

Importantly, such devices can be produced on a large scale because they are simple and easy to manufacture. Hong et al. [115] prepared flexible, free-standing electrochemical RGO/nafion (RGON) hybrid films for organophosphate detection (Fig. 5); they reported that an electrochemical biosensing platform using such a film had high conductivity, low interfacial resistance, a detection limit of 1.37×10^{-7} M, and a rapid response time of < 3 s.

However, RGO-based biosensors have relatively inferior sensitivity owing to the defects caused by impurities resulting from the processes used to produce them [116]. Chemical vapor deposition (CVD) facilitates the production of high-quality graphene and provides control of the number of graphene layers. The graphene surface can be modified with different functional groups via surface engineering. Jang et al. [117] fabricated a liquid ion-gated FET-type flexible graphene aptasensor that was capable of detecting mercury (Hg) with high sensitivity and selectivity (Fig. 6). The sensor device was fabricated by transferring CVD-grown graphene onto a polyethylene naphthalate film with excellent mechanical durability and flexibility. The introduction of an aptamer specific for Hg^{2+} resulted in a flexible graphene-based aptasensor with superior selectivity. Owing to its high electrical conductivity and carrier mobility, the aptasensor had a fast response speed (<1 s) and high sensitivity, with a detection limit of 10 pM. Furthermore, the graphene-based flexible sensor could detect Hg^{2+} in mussels and specifically discriminate Hg^{2+} even in the real complex sample solutions. These results indicate that such graphene-based aptasensors have great potential for detecting Hg in humans and the environment.

Although defect-free graphene with superior electrical conductivity significantly increases detection sensitivity, it can only be used to detect analytes with concentrations higher than the pM level. Graphene-based sensors for the detection of molecules at ultralow concentrations (fM) have been impeded by the intrinsic semi-metal and zero bandgap of graphene [118–120]. The lack of a bandgap results in a negligible current change in response to local environmental disturbances, which limits the fabrication of graphene biosensors with high sensitivity [121]. Therefore, an effective method for opening the bandgap of graphene is in high demand. Jang et al. [116] demonstrated an ultrasensitive and flexible FET bio-electronic nose (B-nose) based on olfactory receptor (OR)-modified, plasma-treated bilayer graphene (Fig. 7). A form of graphene with p- or n-type behavior was created by treatment with oxygen and ammonia plasma. This approach has enabled a moderate bandgap in graphene, which is beneficial for fabricating biosensors with high sensitivity. To provide specificity for the odorant amyl butyrate (AB), the graphene surface was modified with human olfactory receptor 2AG1 (hOR2AG1:OR). The resulting flexible and transparent functionalized graphene B-nose was ultrasensitive and highly selective,

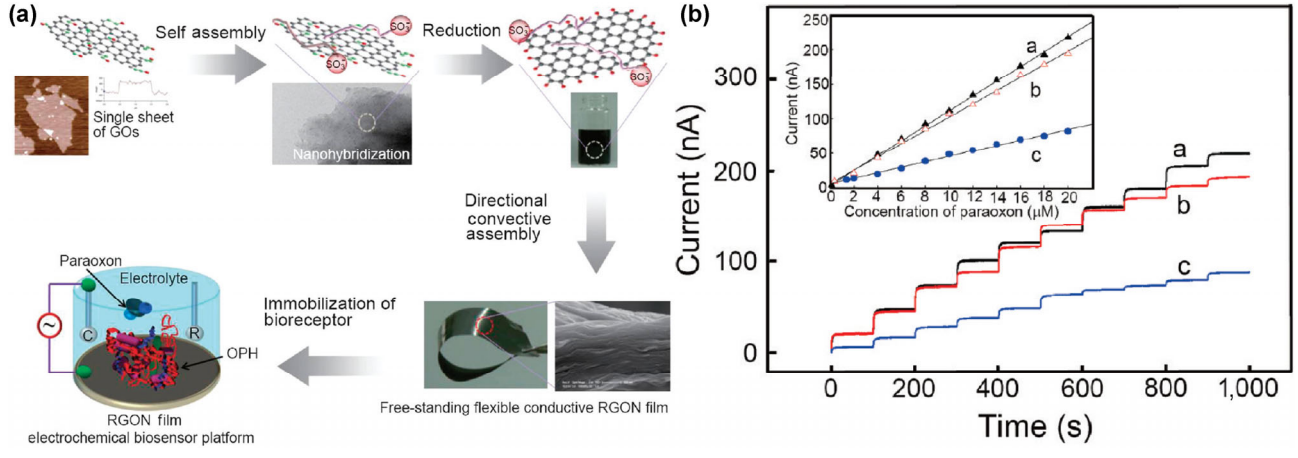

Figure 5 (a) Schematic illustration of the procedure used to design RGON hybrids, and their use in electrochemical biosensors. (b) Amperometric responses with respect to 2 μM increments of paraoxon. a and b: organophosphorus hydrolase (OPH)-modified RGON before and after 100 bending cycles, c: OPH-RGO films. The inset represents the calibration curves of the current signals with respect to the different concentrations of paraoxon. (Reproduced with permission from Ref. [115], © American Chemical Society 2010.)

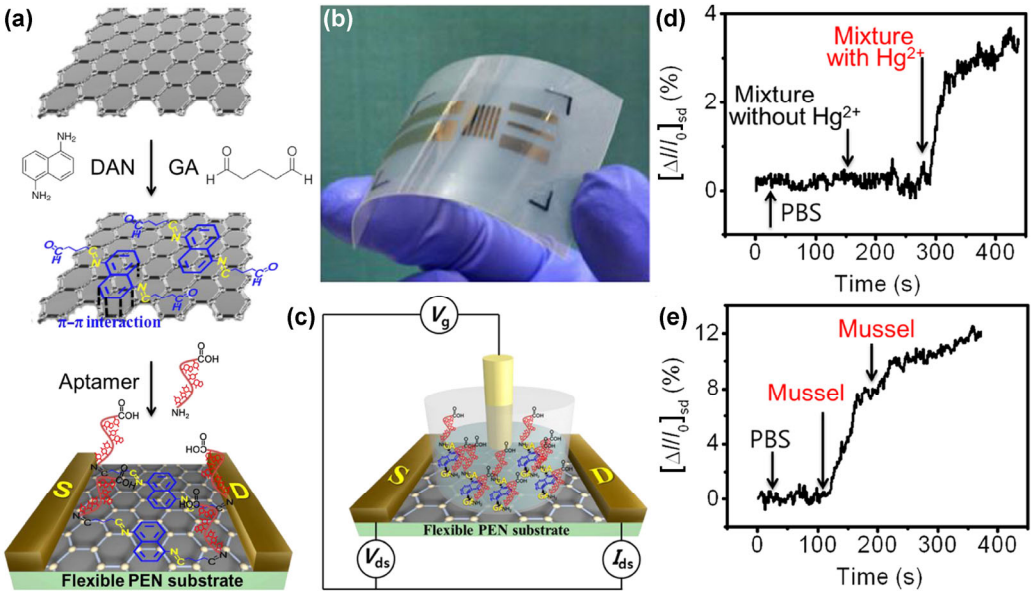

Figure 6 (a) Protocol for the synthesis of a flexible graphene-based aptasensor on a polyethylene naphthalate substrate. (b) Photograph of the flexible and transparent graphene-based sensor device. (c) Schematic illustration of the sensor mechanism for the liquid ion-gated FET biosensor based on graphene. (d) Real-time current responses of graphene-based aptasensor to Hg^{2+}. (e) Real-time current responses of graphene-based aptasensor to exposure to mussel solution. (Reproduced with permission from Ref. [117], © American Chemical Society 2013.)

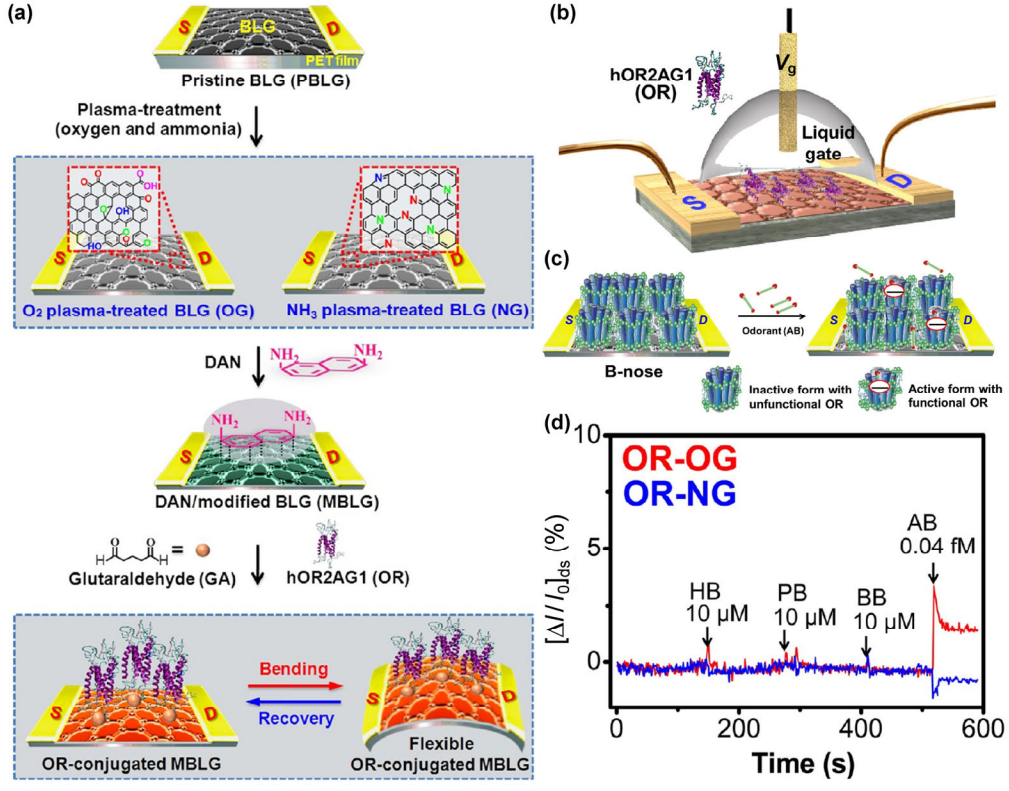

Figure 7 (a) Fabrication process for OR-conjugated B-nose with oxygen and ammonia plasma-treated bilayer graphene. (b) Schematic diagram of the OR-conjugated bilayer graphene-based liquid ion-gated FET B-nose. (c) Schematic illustration of the binding mechanism of B-nose. (d) Current responses of B-nose based on oxygen plasma-treated graphene and ammonia plasma-treated graphene upon addition of nontargets and target odorant. (Reproduced with permission from Ref. [116], © American Chemical Society 2012.)

and could recognize AB with single carbon atom resolution. Furthermore, the flexible B-nose exhibited long-term stability and mechanical bending durability. This method offers a pathway to regulate the bandgap of graphene to obtain high-performance biosensors.

2.3.2 *Transition metal dichalcogenides*

The lack of a bandgap in graphene due to its intrinsic semi-metal performance limits its applicability in logic circuits and biosensors. TMDs offer a large bandgap above 1 eV and have an on/off ratio exceeding seven orders of magnitude [122–127]. Superior mechanical performance arising from a stacked layer structure similar to that of graphene, and a planar arrangement of covalently bonded atoms make TMDs very useful for flexible biosensors. Furthermore, 2D nanomaterials are highly promising for large-scale integrated device processing and fabrication owing to their excellent electrostatic properties and planar structures [128, 129]. Banerjee et al. [130] reported a method for the fabrication of MoS_2-based FET-type pH and protein sensors with high sensitivity (Fig. 8). The mechanical exfoliation method produces MoS_2 with pristine surfaces that are free from out-of-plane pendant bonds; this smooth structure reduces surface scattering and interface traps. Therefore, the MoS_2 FET has high sensitivity to pH change (713 mV/pH) and is highly sensitive to proteins (196 mV/100 fM) compared with graphene-based devices. Theoretical calculations indicate that MoS_2-based biosensors can achieve ultimate scaling

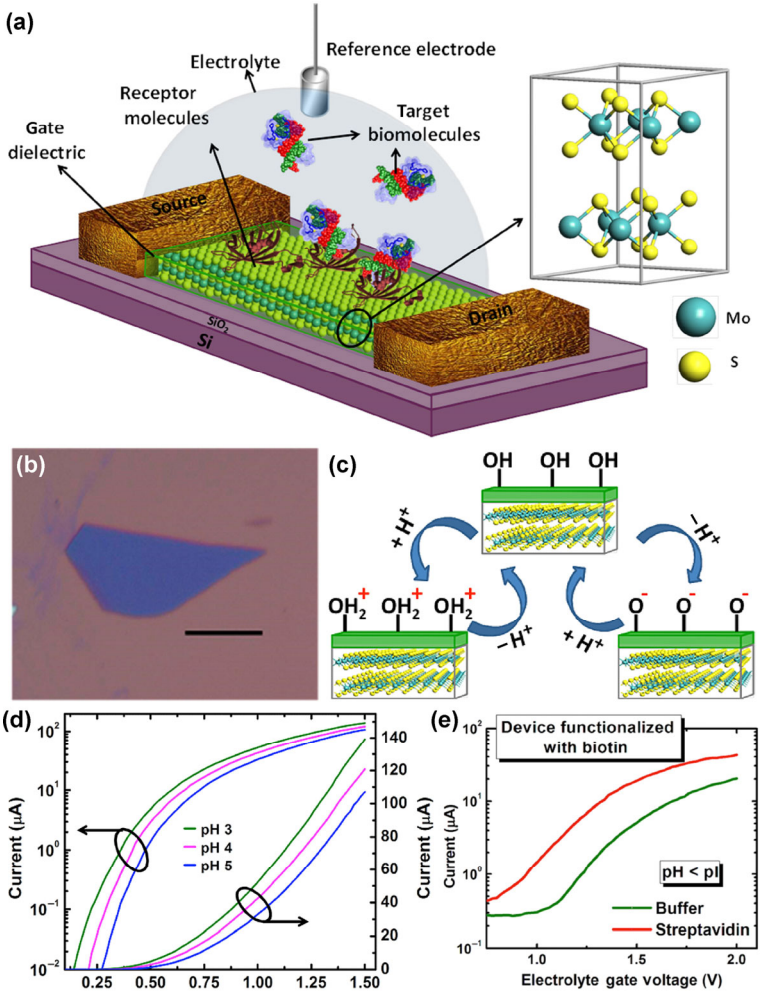

Figure 8 (a) Schematic diagram of MoS_2-based FET biosensor. (b) Optical image of a MoS_2 flake. Scale bar, 10 μm. (c) Illustration of the pH-sensing principle. (d) Drain current as a function of gate voltage for three different pH values. (e) Biotin-functionalized MoS_2 FET biosensor for sensing streptavidin in solution. pI represents the isoelectric point of streptavidin. (Reproduced with permission from Ref. [130], © American Chemical Society 2014.)

limits while retaining high sensitivity. Ultrathin MoS_2 nanosheets are highly transparent, flexible, and mechanically strong. 2D TMDs can be used in wearable and implantable biosensors by interfacing the nanomaterial with flexible substrates. However, the practical application of 2D TMDs in flexible biosensors is problematic because the high temperatures involved in their fabrication may lead to the decomposition of the substrates. Furthermore, carrier mobility on flexible substrates is lower than on Si substrates.

2.4 Composites

The formation of hybrid nanostructures can compensate for the shortcomings of a single material. For instance, graphene/silver nanowire hybrid films not only overcome the limitations of nanowire-percolating networks by decreasing their pattern sizes, the weakness of the nanowire against electrical breakdown, and chemical oxidation, but also decrease the relatively high sheet resistance of graphene [131]. In fluidic sensing devices, pristine graphene has structural limitations such as structural unreliability, irregular active areas, poor adhesion of the fluidic modules, and low sensitivity and selectivity. Therefore, novel technologies for advanced graphene-based hybrids are needed for fabricating high-performance flexible electronics. Lee et al. [132] reported a novel FET biosensor based on RGO-encapsulated nanoparticles for the selective and sensitive detection of key biomarkers of breast cancer. These well-organized 2D or 3D graphene nanostructures with high surface-to-volume ratios can generate 3D electrical surfaces, improving detection limits and facilitating the highly reproducible detection of important biomarkers.

The combination of graphene and nanoparticles provides enlarged active areas that interact with analytes and have a stable sensing geometry. Duan et al. [133] fabricated a new type of flexible electrochemical sensor by depositing high-density Pt nanoparticles on RGO-carrying MnO_2 nanowire networks (Fig. 9). In this well-organized system, RGO serves as the mechanical support and provides high electrical

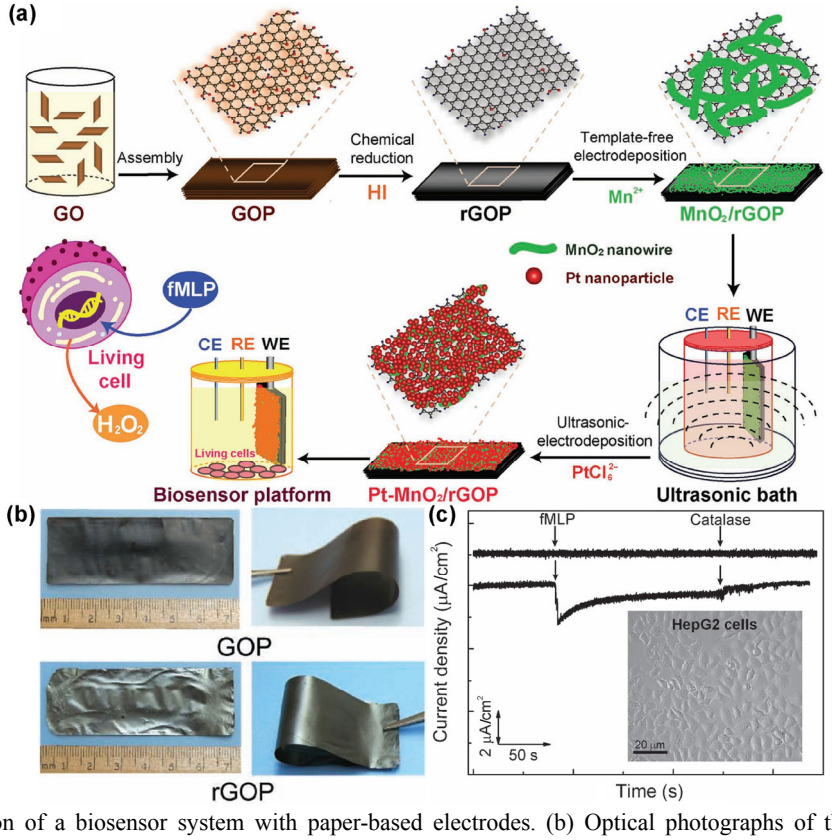

Figure 9 (a) Fabrication of a biosensor system with paper-based electrodes. (b) Optical photographs of the GO and RGO paper. (c) Amperometric responses of the Pt-MnO_2/RGO paper electrode with the addition of fMLP and catalase in the absence (upper) and presence (bottom) of HepG2 cells. Inset, microscopy image of HepG2 cells. (Reproduced with permission from Ref. [133], © John Wiley & Sons 2012.)

conductivity, MnO_2 networks have a high surface area, and Pt nanoparticles have superior catalytic activity. Consequently, the device demonstrated significantly improved sensitivity and selectivity when it was used for the non-enzymatic detection of H_2O_2 secreted by live cells. Jang et al. [134] constructed novel liquid ion-gated FET flexible HIV immunoassays using large-scale graphene micropattern (GM) nanobiohybrids with close-packed carboxylated polypyrrole nanoparticle (cPPyNP) arrays (Fig. 10). Size-controllable graphene micropatterns facilitate the accurate and reliable production of fluidic systems. Owing to the synergistic effect of graphene and the conducting polymer, a nano-biohybrid HIV immunosensor exhibits an unprecedentedly low detection limit of 1 pM. Furthermore, the nano-biohybrid sensor also has excellent mechanical bendability and durability.

3 Device designs

Previously, the developers of flexible biosensors mostly focused on the design of high-sensitivity biosensors with a single modality in which the sensor only measures a unique sensing parameter under a single stimulus. However, in real biological systems multiple variations exist in the micro-environment. Therefore, bio-electronics must be designed to provide multimodality in sensing multiple stimuli. Kim et al. [135] reported a graphene-based wearable electrochemical device for diabetes monitoring and feedback therapy (Fig. 11). The device consists of a sensor system that is composed of temperature, humidity, glucose, and pH sensors. It also includes a therapy system that comprises a heater and polymeric microneedles, which can be thermally activated to deliver drugs transcutaneously. The large-area stretchable device comprises a bilayer of gold mesh and gold-doped graphene with high electrical conductivity and mechanical reliability, which provides the major electrochemical interface for the stable transfer of electrical signals. The sensor for detecting multiple stimuli is produced by selective functionalization of the gold-doped graphene with electrochemically active and soft materials, which enhances the electrochemical

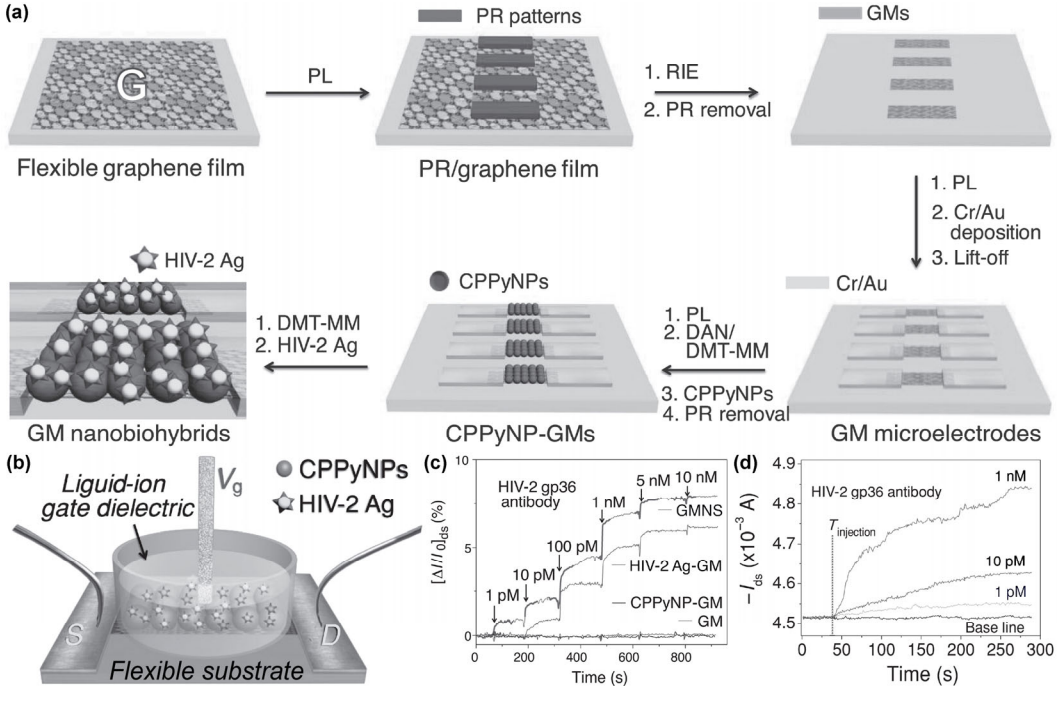

Figure 10 (a) Protocol for the fabrication of flexible FET-type GM nano-biohybrid immunosensor based on GMs conjugated with close-packed CPPyNPs. (b) Schematic illustration of GM nano-biohybrid-based immunosensors (GMNS) operated by liquid gating. (c) Real-time current responses of GM, CPPy-GM, HIV-2 Ag-GM, and GMNS upon exposure to different HIV-2 gp36 Ab concentrations. (d) Current responses of the flexible FET-type GMNS to different HIV-2 gp36 Ab concentrations. (Reproduced with permission from Ref. [134], © John Wiley & Sons 2013.)

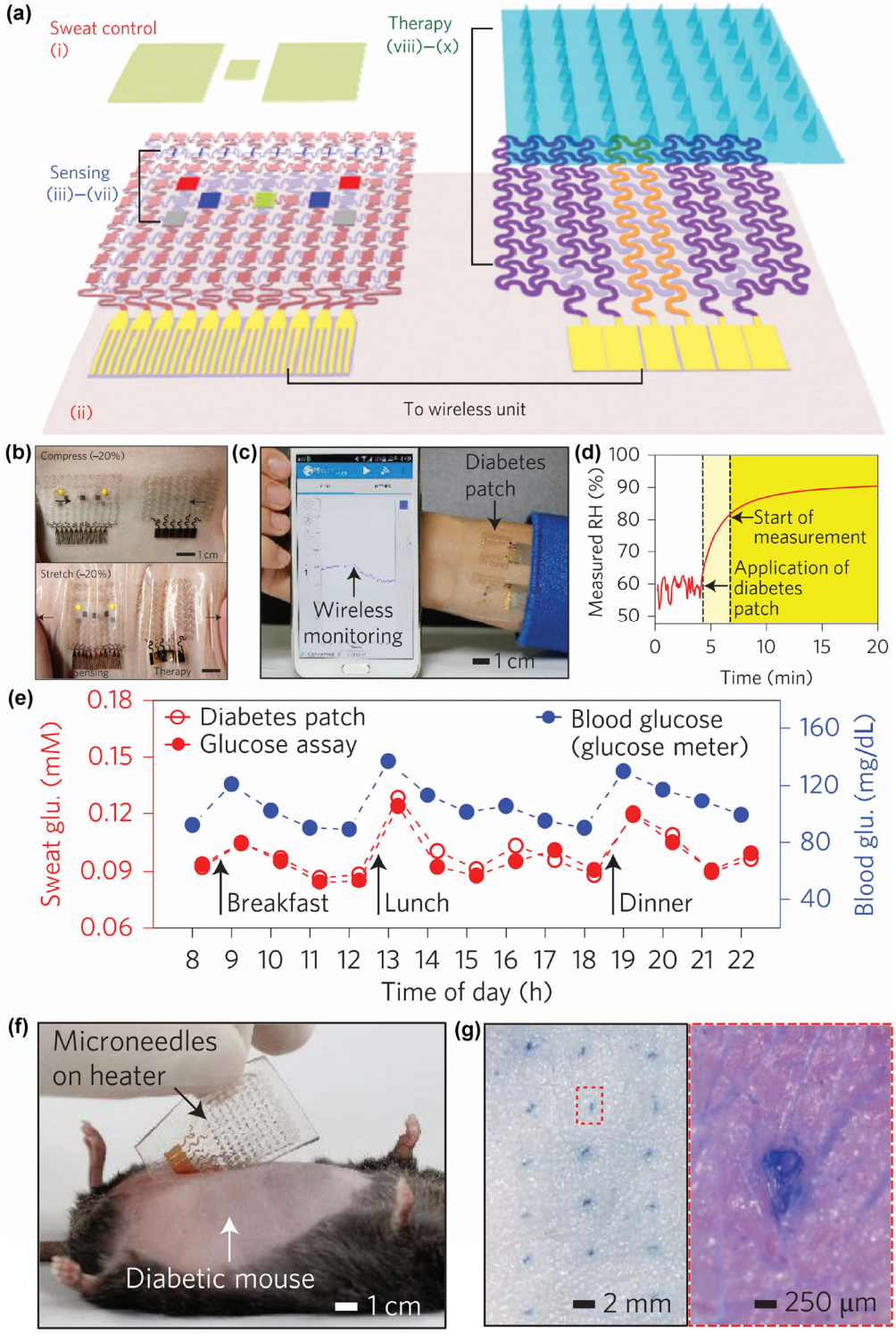

Figure 11 (a) Schematic representation of the diabetes patch with various functional components such as sweat-control, sensing, and therapy systems. (b) Optical camera images of the diabetes patch deposited on human skin with various mechanical deformations. (c) Optical image of a portable electrochemical system connected to the wearable diabetes monitoring and therapy system. (d) Relative humidity measurement by the diabetes patch. (e) Real-time detection of glucose in human sweat and blood with the diabetes patch. (f) Optical image of the heater integrated with microneedles deposited on mouse skin. (g) Optical images of the mouse skin with micro-sized holes. (Reproduced with permission from Ref. [135], © Nature Publishing Group 2016.)

activity and biochemical sensitivity, and retains the intrinsic softness of graphene. The optical transparency of the device ensures a semi-transparent skin-like appearance. Once the sensor is mounted on the human skin, detection begins. Specifically, the sweat uptake layer adsorbs sweat until it reaches a relative humidity of 80%, and then the glucose and pH sensors start to monitor the glucose levels. When hyperglycemia is detected, the thermal actuation of the drug-loaded microneedles begins, releasing the drugs for diabetes therapy. At the same time, the integrated temperature sensor monitors the temperature changes of the skin, and prevents overheating. This multimodality and continuous point-of-care monitoring in combination with thermal actuation therapy based on the electrochemical device provide a unique solution for remote clinical medicine.

Other than multimodality sensing using the same device, an integrated device that is composed of two different electronic systems, in which one serves as the calibration platform to calibrate the electrical signals, is necessary to obtain accurate sensing information. Maharbiz et al. [136] first demonstrated a flexible FET-type electronic sensing device to map pressure-induced tissue damage noninvasively (Fig. 12). The device comprises a multiplexed electrode array with a commercial rigid printed circuit and an inkjet-printed flexible bandage-like array. Here, the rigid device serves as the calibration platform to detect pressure ulcers by impedance spectroscopy, and the flexible device is used for recording the same signal *in vivo*. The whole electronic system is fabricated on a thin, flexible polyethylene naphthalate substrate, significantly enhancing the conformity of the printed array and improving the contact between the electrode and the skin. Mechanical robustness tests indicated that the device arrays can be twisted to 30° for 1,000 cycles. The *in vivo* impedance spectroscopy data from the flexible electrode arrays obtained from a rat model indicated that impedance is robustly correlated with tissue health. This device design demonstrates the feasibility of an automated, noninvasive "smart bandage" for the early diagnosis of pressure ulcers.

4 Integrated sensor platforms

4.1 Wearable self-powered devices

Flexible electronic sensors require a sustainable power source [43, 137, 138]. Traditional large and rigid power sources have certain limitations: They are inconvenient to operate and have indispensable wire connections, which are a disadvantage in flexible electronics. In this regard, the integration of a power generator with

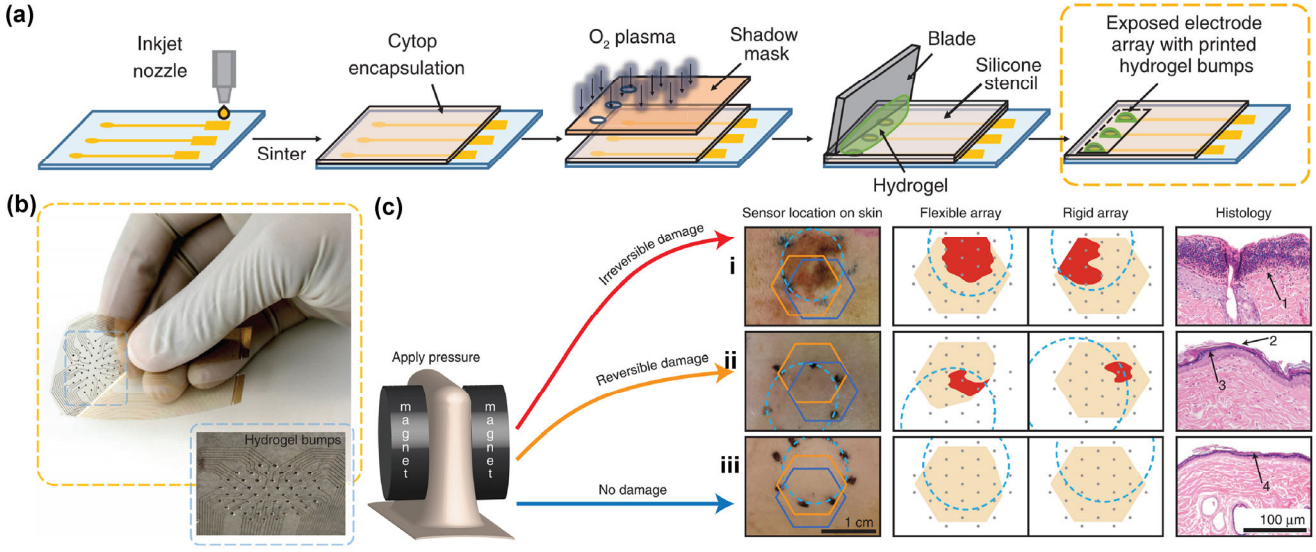

Figure 12 (a) Fabrication processes of the inkjet printed flexible electrode array. (b) Photograph of an inkjet printed array. Inset is the printed hydrogel bumps. (c) Early detection of pressure-induced tissue damage with different degrees of damage. (Reproduced with permission from Ref. [137], © Nature Publishing Group 2015.)

a flexible biosensor is an efficient design for wearable self-powered devices. The mechanical energy derived from various stretching motions is a cost-effective and highly efficient approach to energy harvesting.

Wang et al. [139] fabricated a flexible triboelectric nanogenerator (FTENG) by assembling serpentine-patterned electrodes with a wavy-structured Kapton film on an elastic PDMS substrate (Fig. 13). The unique design of the structure enables the FTENG to operate under both compressive and stretching conditions, and it can be conformably attached to human skin for detecting the gentle motions of joints and muscles. As a result, the FTENG enables high-output power density (5 W/cm^2), and can be stretched up to a tensile strain of 22% without loss of performance. This research presents an unprecedented development in energy harvesting and self-powered sensors, and offers a guideline for the next generation of flexible electronics and bio-integrated systems.

In addition to triboelectric nanogenerators, piezoelectric devices can be used to harvest energy from external pressure. Wang et al. [140] reported a new approach for the fabrication of flexible fiber nanogenerators (FNGs), and investigated their use in flexible electronics and medical diagnosis (Fig. 14). The FNGs comprise pressure-sensitive zinc oxide (ZnO) thin films coated on flexible carbon fibers. When it is subjected to uni-compression, the ZnO film generates a macroscopic piezopotential, which results in an electric current in the external load. The output peak voltage and average current density can reach 3.2 V and 0.15 μA/cm^2, respectively. Because the FNGs rely on air pressure, they can work in a non-contact mode such as in rotating tires, flowing air/liquid, or even in blood vessels. This flexible piezoelectric generator can also be used for ultrasensitive monitoring of the pressure derived from the human heart, suggesting its potential use in sensors for medical diagnosis and in measurement tools.

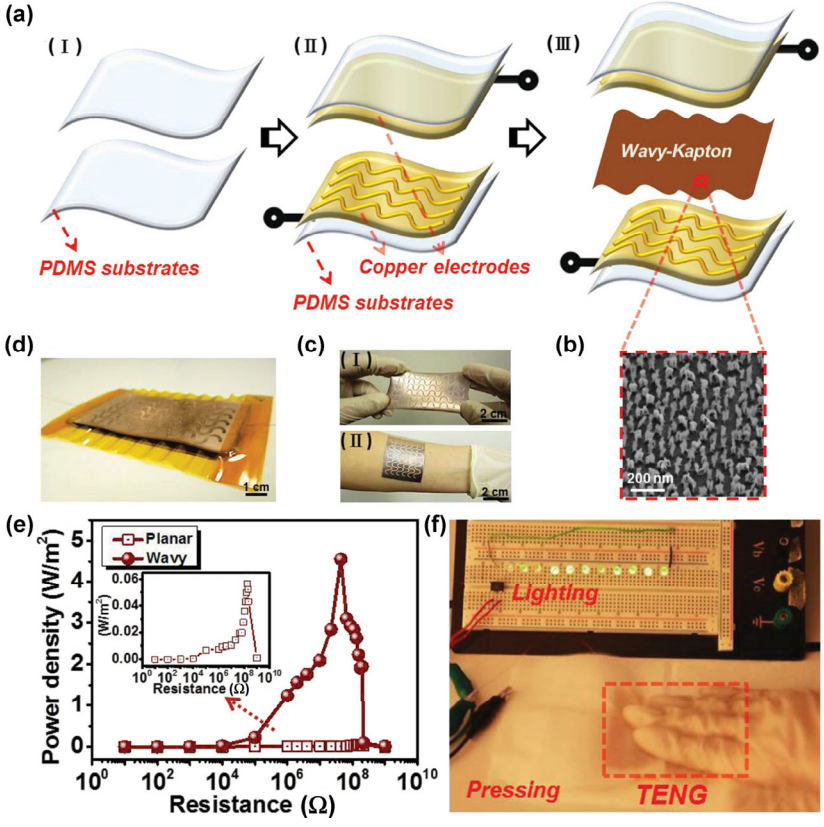

Figure 13 (a) Schematic of the wavy-FTENG device structure. (b) SEM image of nanowire on the Kapton film surface. (c) Photographs of the flexible serpentine-patterned electrodes on human skin and under stretching deformation. (d) Photograph of the flexible wavy-FTENG device. (e) Power density versus resistance of the external load based on planar-TENG and wavy-FTENG, respectively. (f) Photograph of 10 commercial green LEDs, which were driven by the wavy-FTENG. (Reproduced with permission from Ref. [139], © John Wiley and Sons 2015.)

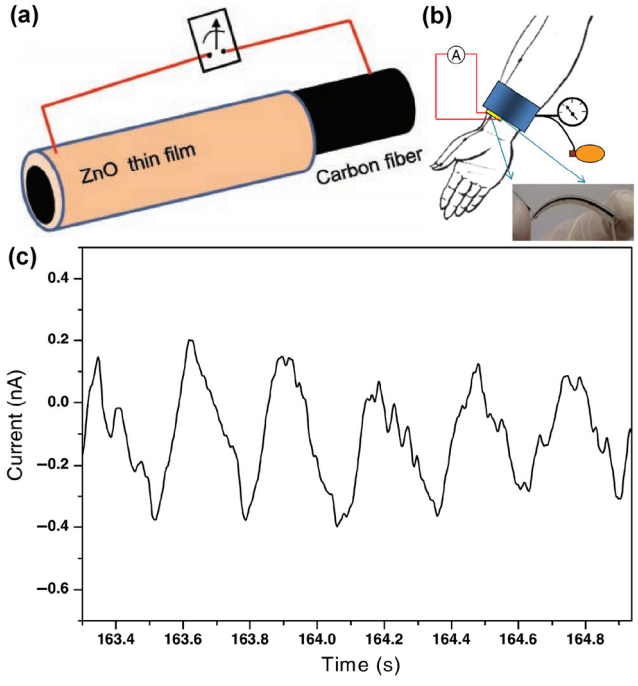

Figure 14 (a) Schematic of a fiber nanogenerator, which was fabricated by coating a ZnO thin film onto carbon fiber. (b) Schematics of the experimental set-up. (c) The electric current outputs of a FNG exposed to heartbeat pulses. (Reproduced with permission from Ref. [140], © John Wiley & Sons 2011.)

4.2 Data processing systems

The fabrication of high-performance and energy-efficient sensors with memory modules, and the development of controlled-delivery therapeutic systems that continuously monitor key physiological parameters, store data, and deliver feedback therapy are the next frontiers in personalized medicine and healthcare [30, 31]. However, multimodal detection and therapy remain a great challenge because sophisticated fabrication processes such as photolithography and printing are needed to enable large-area integration of sensor arrays with different sensing functions in a single system. Kim et al. [32] addressed these challenges by the monolithic integration of nanomembranes, nanoparticles, and stretchable electronics on a tissue-like polymeric substrate (Fig. 15). This bio-integrated system includes physiological sensors, non-volatile memory, and drug-release actuators. As shown in Fig. 15, movement disorders can be monitored using a Si nanomembrane strain sensor, and the resulting data can be stored in gold nanoparticle memory devices. The stored data are then analyzed and feedback therapy is affected by thermal stimuli, releasing drugs from mesoporous silica nanoparticles. Importantly, the drug delivery rate and amount are continuously controlled by a temperature sensor to prevent skin burns. This design principle of sensing, memory, and therapeutic modules provides a concept for the development of electronic devices that include energy storage units, central control units such as microprocessors, and wireless monitoring elements for achieving remote personal healthcare.

4.3 Wireless biosensors

Traditionally, interfacing electronic devices with biomaterials always involves either implantation of device electrodes into tissue or mechanical mounting of components on the body. The rigid, bulky onboard power sources, associated circuitry, and connections between sensing probes with data processing electronics significantly increase the device mass and impede the development of point-of-use and implantable electronics. Furthermore, the rigid substrates prohibit the intimate contact between the sensor component and curvilinear biological tissues. In this regard, device designs for minimizing the size of the power source or constructing wireless electronics are highly desired for conformal bio-integrated electronics and sensors [141, 142]. Nanomaterials such as CNTs, graphene, conducting polymers, and composites have been used to fabricate wireless chemical and gas sensors [40, 143, 144]. Bao et al. [145] reported a wireless, real-time pressure sensing system with passive, flexible, millimeter-scale sensors with dimensions down to 1 mm × 1 mm × 0.1 mm to capture human pulse waveforms wirelessly, and to simultaneously and continuously monitor intracranial pressure (Fig. 16). The sensor device was composed of a pressure-sensitive capacitive element called a microstructured styrene–butadiene–styrene elastomer sandwiched by two printed copper inductive antenna on a PI substrate to form a resonant circuit. This unique sandwich structure is used to minimize the size of the sensor and overcome the limitations in operating frequency of traditional passive strategies. Once pressure is applied, the distance between the spiral layers is narrowed, and the coupling capacitance is increased. Additionally, the resonant frequency also shifts down

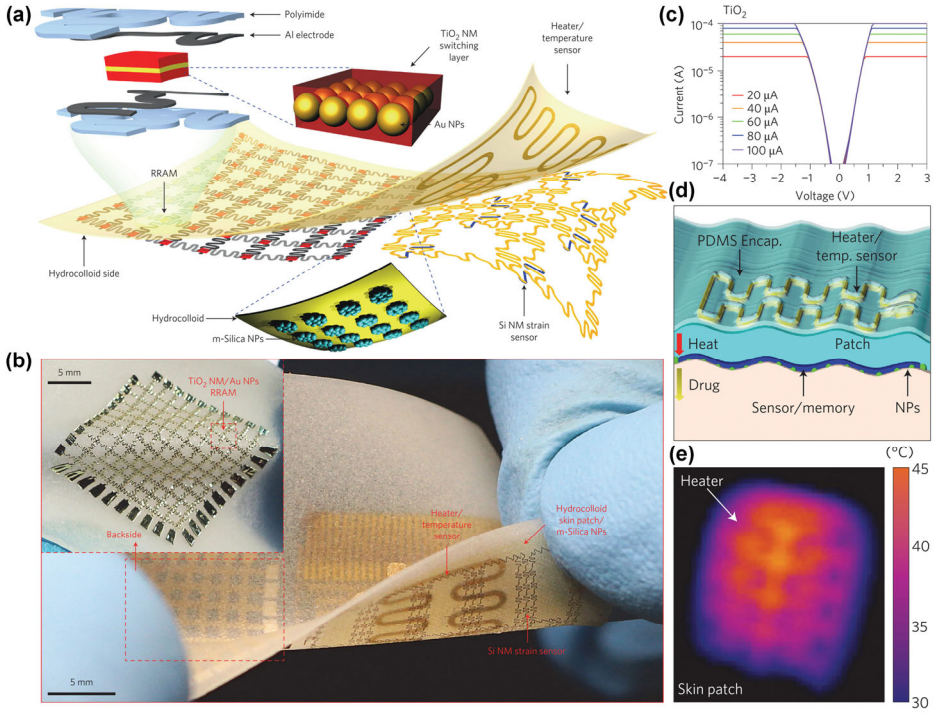

Figure 15 (a) Wearable electronic patch with data storage modules, diagnostic tools, and therapeutic actuating elements. (b) Optical image of the wearable bio-integrated system. (c) Current versus voltage characteristics with compliance currents below ~100 μA. (d) Schematic representation of the controlled transdermal drug delivery patch. (e) Temperature distribution of the heater on the skin patch. (Reproduced with permission from Ref. [32], © Nature Publishing Group 2014.)

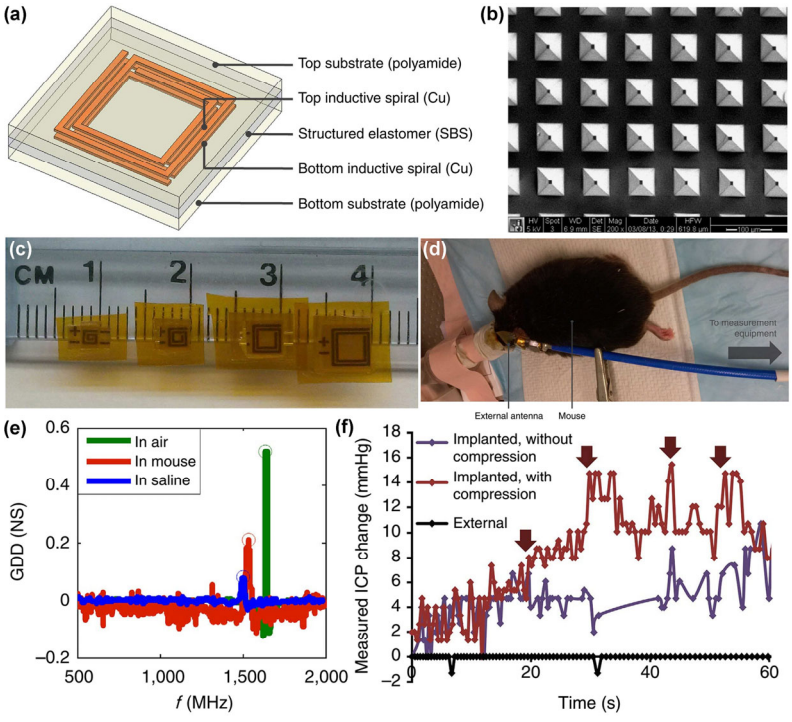

Figure 16 (a) Structure design of the resonant sensor device. (b) Photograph of the pyramidal-structured SBS dielectric. (c) Photograph of the 2-turn devices with different dimensions. (d) Wireless monitoring with the sensor implanted in mouse. (e) The sensor resonant peak in the measured group delay distortion (GDD) spectrum under no applied air pressure, saline, and mouse. (f) Measured pressure waveforms after performing abdominal compression on mouse. An external reference sensor was also used. Arrows indicate when compression was applied. (Reproduced with permission from Ref. [145], © Nature Publishing Group 2014.)

to lower frequencies under a specific pressure. This uniquely designed small and flexible device with improved mechanical robustness allows the intimate connection of sensors with biomaterials. The wireless sensor arrays can continuously capture human pulse waveforms *in vivo* with high sensitivity, and can obtain concurrent spatial pressure mapping. This fabrication technology has enabled a range of applications in continuous and wireless detection of various important physiological parameters for biomedical research and human healthcare.

5 Issues and challenges

Despite the outstanding properties of nanostructured material for advanced bio-electronics and integrated devices, it is prudent to give a comprehensive discussion of the challenges that flexible electronics have faced. In terms of the material synthesis, the exploration of a large-scale and highly efficient approach towards patterned nanomaterials is of vital importance for the fabrication of flexible devices with high sensitivity and reproducibility. However, the engineering of 0D nanomaterials with superior contact to improve the conductivity and reduce the power consumption remains a practical challenge. Interconnected 1D nanomaterials exhibit high conductivity, even when stretched. However, nanowires are not widely utilized in devices owing to the limitations of reproducibility and stability [146–148]. High-performance nanowire-based devices always require complex and difficult fabrication processes. More importantly, for practical flexible nanoelectronics, the large area pattering of 2D thin films and devices on flexible substrates is an essential prerequisite. Though some techniques based on sheet and roll-to-roll processing for large-area nanotechnology have been explored, obtaining large-area and high-quality 2D nanomaterials has significantly impeded the commercialization of the current flexible devices [149–151].

The surface modifications of nanomaterials with specific recognition elements are convincing solutions to satisfy the required selectivity, sensitivity, and stability of biosensors. Thus, surface modification technologies that do not influence the electronic and physical performance of nanomaterials are desired. The long-term toxicity analysis of nanomaterials is also critical for invasive bioelectronics. In addition, the selectivity and long-term stability of biosensors in practical or complex environments must be considered. The engineering of functionalized nanomaterial arrays to facilitate the fabrication of multifunctional microchips for highly efficient, sensitive, and selective sensing are of critical importance for real-time analysis. It is worth mentioning that the surface functionalization of nanomaterials to provide hydrophilicity can also significantly enhance the contact between the device and biomaterials, and thus improve biosensing performance.

In real-life applications of flexible biosensors for disease diagnosis, the exploitation of integrated systems such as the combination of physical and chemical or biological sensors for monitoring multiplex motions and disease biomarkers are essential. In particular, the integration of sensors with data storage systems and transmission systems for long-term and continuous monitoring, delivering signals to an instrument for further analysis, transferring feedback information to humans, and providing the corresponding therapies is a goal for personal healthcare. However, the combination of each device component to realize fully integrated flexible bio-electronics remains a challenge. More importantly, the sophisticated preparation procedures involving photolithography and printing to obtain large-area sensor arrays, power sources, and wireless monitoring systems remains to be addressed for practical implementation. Currently developed energy harvesting and storage devices that provide the energy to power electronic devices are typically heavy owing to the presence of bulk and rigid cell encapsulation material. The mass loading of active material in electrodes must be kept at a relatively high value to obtain high energy and power density, which significantly impedes the realization of transparent batteries [152–157]. Therefore, it is difficult to integrate energy storage systems with whole bio-electronics because flexible and wearable bio-electronics require characteristics such as low weight and transparency. Although devices that provide detection and therapy facilitate a pathway for point-of-care medicine, the low drug loading capacity of such devices makes disease therapy difficult [32, 135]. Furthermore, detection and therapy devices that can only be used once

owing to the difficulty of cleaning the device surface, significantly increase the fabrication costs.

6 Conclusions and outlook

Over the past decade, advances in nanostructured materials, mechanical analysis, surface engineering, device design, and nanofabrication techniques have accelerated the development of flexible bio-electronics. We have summarized the most recent developments in flexible biosensors from the perspective of various nanostructured nanomaterials and integrated device systems. This review will provide researchers with information on material selection, sensor fabrication, data processing, and power requirements for flexible biosensors. However, there are several remaining challenges for the effective integration of these nanomaterials with soft substrates to obtain flexible bio-electronics. The optimization of material fabrication and modification techniques to obtain large-area, high quality, and uniform arrays is essential for the fabrication of highly sensitive and reproducible biosensors. The exploration of small energy storage and conversion devices with high energy and power density, and optical transparency is important for the development of high-performance bio-electronics. Furthermore, device integration should be optimized to minimize the whole device volume for implantable electronics and point-of-care healthcare.

Acknowledgements

This work was supported by the National Natural Science Foundation of China (Nos. 51272186, 21422105, and 21675120), the Foundation for the Author of National Excellent Doctoral Dissertation of PR China (No. 201220), and Ten Thousand Talents Program for Young Talents.

References

[1] Gao, W.; Emaminejad, S.; Nyein, H. Y. Y.; Challa, S.; Chen, K.; Peck, A.; Fahad, H. M.; Ota, H.; Shiraki, H.; Kiriya, D. et al. Fully integrated wearable sensor arrays for multiplexed *in situ* perspiration analysis. *Nature* **2016**, *529*, 509–526.

[2] Tee, B. C.-K.; Wang, C.; Allen, R.; Bao, Z. N. An electrically and mechanically self-healing composite with pressure- and flexion-sensitive properties for electronic skin applications. *Nat. Nanotechnol.* **2012**, *7*, 825–832.

[3] Park, S.; Wang, G.; Cho, B.; Kim, Y.; Song, S.; Ji, Y.; Yoon, M.-H.; Lee, T. Flexible molecular-scale electronic devices. *Nat. Nanotechnol.* **2012**, *7*, 438–442.

[4] Trung, T. Q.; Lee N.-E. Flexible and stretchable physical sensor integrated platforms for wearable human-activity monitoring and personal healthcare. *Adv. Mater.* **2016**, *28*, 4338–4372.

[5] Viventi, J.; Kim, D.-H.; Vigeland, L.; Frechette, E. S.; Blanco, J. A.; Kim, Y.-S.; Avrin, A. E.; Tiruvadi, V. R.; Hwang, S.-W.; Vanleer, A. C. et al. Flexible, foldable, actively multiplexed, high-density electrode array for mapping brain activity *in vivo*. *Nat. Neurosci.* **2011**, *14*, 1599–1607.

[6] Nguyen, T. D.; Deshmukh, N.; Nagarah, J. M.; Kramer, T.; Purohit, P. K.; Berry M. J.; McAlpine, M. C. Piezoelectric nanoribbons for monitoring cellular deformations. *Nat. Nanotechnol.* **2012**, *7*, 587–593.

[7] Rim, Y. S.; Bae, S.-H.; Chen, H. J.; De Marco, N.; Yang, Y. Recent progress in materials and devices toward printable and flexible sensors. *Adv. Mater.* **2016**, *28*, 4415–4440.

[8] Khan, Y.; Ostfeld, A. E.; Lochner, C. M.; Pierre, A.; Arias, A. C. Monitoring of vital signs with flexible and wearable medical devices. *Adv. Mater.* **2016**, *28*, 4373–4395.

[9] Salvatore, G. A.; Münzenrieder, N.; Kinkeldei, T.; Petti, L.; Zysset, C.; Strebel, I.; Büthe, L.; Tröster, G. Wafer-scale design of lightweight and transparent electronics that wraps around hairs. *Nat. Commun.* **2014**, *5*, 2982.

[10] Mannsfeld, S. C. B.; Tee, B. C.-K.; Stoltenberg, R. M.; Chen, C. V. H.-H.; Barman, S.; Muir, B. V. O.; Sokolov, A. N. Reese, C.; Bao, Z. N. Highly sensitive flexible pressure sensors with microstructured rubber dielectric layers. *Nat. Mater.* **2010**, *9*, 859–864.

[11] Lee, S.; Reuveny, A.; Reeder, J.; Lee, S.; Jin, H.; Liu, Q. H.; Yokota, T.; Sekitani, T.; Isoyama, T.; Abe, Y. et al. A transparent bending-insensitive pressure sensor. *Nat. Nanotechnol.* **2016**, *11*, 472–478.

[12] Ramuz, M.; Tee, B. C.-K.; Tok, J. B.-H.; Bao, Z. N. Transparent, optical, pressure-sensitive artificial skin for large-area stretchable electronics. *Adv. Mater.* **2012**, *24*, 3223–3227.

[13] Jung, S.; Lee, J.; Hyeon, T.; Lee, M.; Kim, D.-H. Fabric-based integrated energy devices for wearable activity monitors. *Adv. Mater.* **2014**, *26*, 6329–6334.

[14] Pang, C.; koo, J. H.; Nguyen, A.; Caves, J. M.; Kim, M.-G.; Chortos, A.; Kim, K.; Wang, P. J.; Tok, J. B.-H.; Bao, Z. N. Highly skin-conformal microhairy sensor for pulse signal amplification. *Adv. Mater.* **2015**, *27*, 634–640.

[15] Kim, J.; Lee, M.; Shim, H. J.; Ghaffari, R.; Cho, H. R.; Son, D.; Jung, Y. H.; Soh, M.; Choi, C.; Jung, S. et al. Stretchable silicon nanoribbon electronics for skin prosthesis. *Nat. Commun.* **2014**, *5*, 5747.

[16] Kim, R.-H.; Kim, D.-H.; Xiao, J. L.; Kim, B. H.; Park, S.-I.; Panilaitis, B.; Ghaffari, R.; Yao, J. M.; Li, M.; Liu, Z. J. et al. Waterproof AlInGaP optoelectronics on stretchable substrates with applications in biomedicine and robotics. *Nat. Mater.* **2010**, *9*, 929–937.

[17] Guo, Y. L.; Wu, B.; Liu, H. T.; Ma, Y. Q.; Yang, Y.; Zheng, J.; Gui, Y.; Liu, Y. Q. Electrical assembly and reduction of graphene oxide in a single solution step for use in flexible sensors. *Adv. Mater.* **2011**, *23*, 4626–4630.

[18] Dong, X. C.; Shi, Y. M.; Huang, W.; Chen, P.; Li, L.-J. Electrical detection of DNA hybridization with single-base specificity using transistors based on CVD-grown graphene sheets. *Adv. Mater.* **2010**, *22*, 1649–1653.

[19] Xu, G. Y.; Abbott, J.; Qin, L.; Yeung, K. Y. M.; Song, Y.; Yoon, H. S.; Kong, J.; Ham, D. Electrophoretic and field-effect graphene for all-electrical DNA array technology. *Nat. Commun.* **2014**, *5*, 4866.

[20] He, Q. Y.; Sudibya, H. G.; Yin, Z. Y.; Wu, S. X.; Li, H.; Boey, F.; Huang, W.; Chen, P.; Zhang, H. Centimeter-long and large-scale micropatterns of reduced graphene oxide films: Fabrication and sensing applications. *ACS Nano* **2010**, *4*, 3201–3208.

[21] Feng, L. Y.; Chen, Y.; Ren, J. S.; Qu, X. G. A graphene functionalized electrochemical aptasensor for selective label-free detection of cancer cells. *Biomaterials* **2011**, *32*, 2930–2937.

[22] Zhang, M.; Liao, C. Z.; Mak, C. H.; You, P.; Mak, C. L.; Yan, F. Highly sensitive glucose sensors based on enzyme-modified whole-graphene solution-gated transistors. *Sci. Rep.* **2015**, *5*, 8311.

[23] Zhang, M.; Liao, C. Z.; Yao, Y. L.; Liu, Z. K.; Gong, F. F.; Yan, F. High-performance dopamine sensors based on whole-graphene solution-gated transistors. *Adv. Funct. Mater.* **2014**, *24*, 978–985.

[24] Yan, F.; Zhang, M.; Li, J. H. Solution-gated graphene transistors for chemical and biological sensors. *Adv. Healthc. Mater.* **2014**, *3*, 313–331.

[25] Deng, W.; Zhang, X. J.; Huang, L. M.; Xu, X. Z.; Wang, L.; Wang, J. C.; Shang, Q. X.; Lee, S.-T.; Jie, J. S. Aligned single-crystalline perovskite microwire arrays for high-performance flexible image sensors with long-term stability. *Adv. Mater.* **2016**, *28*, 2201–2208.

[26] Shin, S. R.; Farzad, R.; Tamayol, A.; Manoharan, V.; Mostafalu, P.; Zhang, Y. S.; Akbari, M.; Jung, S. M.; Kim, D.; Comotto, M. et al. A bioactive carbon nanotube-based ink for printing 2D and 3D flexible electronics. *Adv. Mater.* **2016**, *28*, 3280–3289.

[27] Bhattacharyya, D.; Senecal, K.; Marek, P.; Senecal, A.; Gleason, K. K. High surface area flexible chemiresistive biosensor by oxidative chemical vapor deposition. *Adv. Funct. Mater.* **2011**, *21*, 4328–4337.

[28] Baeg, K.-J.; Caironi, M.; Noh, Y.-Y. Toward printed integrated circuits based on unipolar or ambipolar polymer semiconductors. *Adv. Mater.* **2013**, *25*, 4210–4244.

[29] Chen, H. T.; Cao, Y.; Zhang, J. L.; Zhou, C. W. Large-scale complementary macroelectronics using hybrid integration of carbon nanotubes and IGZO thin-film transistors. *Nat. Commun.* **2014**, *5*, 4097.

[30] Chen, H. L.; Cheng, N. Y.; Ma, W.; Li, M. L.; Hu, S. X.; Gu, L.; Meng, S.; Guo, X. F. Design of a photoactive hybrid bilayer dielectric for flexible nonvolatile organic memory transistors. *ACS Nano* **2016**, *10*, 436–445.

[31] Kim, R. H.; Kim, H. J.; Bae, I.; Hwang, S. K.; Velusamy, D. B.; Cho, S. M.; Takaishi, K.; Muto, T.; Hashizume, D.; Uchiyama, M. et al. Non-volatile organic memory with sub-millimetre bending radius. *Nat. Commun.* **2014**, *5*, 3583.

[32] Son, D.; Lee, J.; Qiao, S. T.; Ghaffari, R.; Kim, J.; Lee, J. E.; Song, C.; Kim, S. J.; Lee, D. J.; Jun, S. W. et al. Multifunctional wearable devices for diagnosis and therapy of movement disorders. *Nat. Nanotechnol.* **2014**, *9*, 397–404.

[33] Irimia-Vladu, M.; Troshin, P. A.; Reisinger, M.; Shmygleva, L.; Kanbur, Y.; Schwabegger, G.; Bodea, M.; Schwödiauer, R.; Mumyatov, A.; Fergus, J. W. et al. Biocompatible and biodegradable materials for organic field-effect transistors. *Adv. Funct. Mater.* **2010**, *20*, 4069–4076.

[34] Takahashi, T.; Takei, K.; Gillies, A. G.; Fearing, R. S.; Javey, A. Carbon nanotube active-matrix backplanes for conformal electronics and sensors. *Nano Lett.* **2011**, *11*, 5408–5413.

[35] Lau, P. H.; Takei, K.; Wang, C.; Ju, Y.; Kim, J.; Yu, Z. B.; Takahashi, T.; Cho, G.; Javey, A. Fully printed, high performance carbon nanotube thin-film transistors on flexible substrates. *Nano Lett.* **2013**, *13*, 3864–3869.

[36] Chae, S. H.; Yu, W. J.; Bae, J. J.; Duong, D. L.; Perello, D.; Jeong, H. Y.; Ta, Q. H.; Ly, T. H.; Vu, Q. A.; Yun, M. et al. Transferred wrinkled Al_2O_3 for highly stretchable and transparent graphene–carbon nanotube transistors. *Nat. Mater.* **2013**, *12*, 403–409.

[37] Wang, X. W.; Gu, Y.; Xiong, Z. P.; Cui, Z.; Zhang, T. Silk-molded flexible, ultrasensitive, and highly stable electronic skin for monitoring human physiological signals. *Adv. Mater.* **2014**, *26*, 1336–1342.

[38] Segev-Bar, M.; Haick, H. Flexible sensors based on nanoparticles. *ACS Nano* **2013**, *7*, 8366–8378.

[39] Zhu, B. W.; Wang, H.; Leow, W. R.; Cai, Y. R.; Loh, X. J.; Han, M.-Y.; Chen, X. D. Silk fibroin for flexible electronic devices. *Adv. Mater.* **2016**, *28*, 4250–4265.

[40] Mannoor, M. S.; Tao, H.; Clayton, J. D.; Sengupta, A.; Kaplan, D. L.; Naik, R. R.; Verma, N.; Omenetto, F. G.; McAlphine, M. C. Graphene-based wireless bacteria detection on tooth enamel. *Nat. Commun.* **2012**, *3*, 763.

[41] Lee, H.; Choi, T. K.; Lee, Y. B.; Cho, H. R.; Ghaffari, R.; Wang, L.; Choi, H. J.; Chung, T. D.; Lu, N. S.; Hyeon, T. et al. A graphene-based electrochemical device with thermoresponsive microneedles for diabetes monitoring and therapy. *Nat. Nanotechnol.* **2016**, *11*, 566–572.

[42] Swisher, S. L.; Lin, M. C.; Liao, A.; Leeflang, E. J.; Khan, Y.; Pavinatto, F. J.; Mann, K.; Naujokas, A.; Young, D.; Roy, S. et al. Impedance sensing device enables early detection of pressure ulcers *in vivo*. *Nat. Commun.* **2015**, *6*, 6575.

[43] Wang, X. D.; Zhang, H. L.; Yu, R. M.; Dong, L.; Peng, D. F.; Zhang, A. H.; Zhang, Y.; Liu, H.; Pan, C. F.; Wang, Z. L. Dynamic pressure mapping of personalized handwriting by a flexible sensor matrix based on the mechanoluminescence process. *Adv. Mater.* **2015**, *27*, 2324–2331.

[44] Khodagholy, D.; Rivnay, J.; Sessolo, M.; Gurfinkel, M.; Leleux, P.; Jimison, L. H.; Stavrinidou, E.; Herve, T.; Sanaur, S.; Owens, R. M. et al. High transconductance organic electrochemical transistors. *Nat. Commun.* **2013**, *4*, 2133.

[45] Rim, Y. S.; Bae, S.-H.; Chen, H. J.; Yang, J. L.; Kim, J.; Andrews, A. M.; Weiss, P. S.; Yang, Y.; Tseng, H.-R. Printable ultrathin metal oxide semiconductor-based conformal biosensors. *ACS Nano* **2015**, *9*, 12174–12181.

[46] Liu, J.; Buchholz, B.; Chang, R. P. H.; Facchetti, A.; Marks, T. J. High-performance flexible transparent thin-film transistors using a hybrid gate dielectric and an amorphous zinc indium tin oxide channel. *Adv. Mater.* **2010**, *22*, 2333–2337.

[47] Lu, X. H.; Zhai, T.; Zhang, X. H.; Shen, Y. Q.; Yuan, L. Y.; Hu, B.; Gong, L.; Chen, J.; Gao, Y. H.; Zhou, J. et al. WO_{3-x}@Au@MnO_2 core–shell nanowires on carbon fabric for high-performance flexible supercapacitors. *Adv. Mater.* **2012**, *24*, 938–944.

[48] Lin, P.; Luo, X. T.; Hsing, I.-M.; Yan, F. Organic electrochemical transistors integrated in flexible microfluidic systems and used for label-free DNA sensing. *Adv. Mater.* **2011**, *23*, 4035–4040.

[49] Bavykin, D. V.; Friedrich, J. M.; Walsh, F. C. Protonated titanates and TiO_2 nanostructured materials: Synthesis, properties, and applications. *Adv. Mater.* **2006**, *18*, 2807–2824.

[50] Wu, C. Z.; Wei, H.; Ning, B.; Xie, Y. New vanadium oxide nanostructures: Controlled synthesis and their smart electrical switching properties. *Adv. Mater.* **2010**, *22*, 1972–1976.

[51] Yan, J. Q.; Wang, T.; Wu, G. J.; Dai, W. L.; Guan, N. J.; Li, L. D.; Gong, J. L. Tungsten oxide single crystal nanosheets for enhanced multichannel solar light harvesting. *Adv. Mater.* **2015**, *27*, 1580–1586.

[52] Pradhan, D.; Noroui, F.; Leung, K. T. High-performance, flexible enzymatic glucose biosensor based on ZnO nanowires supported on a gold-coated polyester substrate. *ACS Appl. Mater. Interfaces* **2010**, *2*, 2409–2412.

[53] Liu, X.; Gu, L. L.; Zhang, Q. P.; Wu, J. Y.; Long, Y. Z.; Fan, Z. Y. All-printable band-edge modulated ZnO nanowire photodetectors with ultra-high detectivity. *Nat. Commun.* **2014**, *5*, 4007.

[54] Kim, M.-G.; Kanatzidis, M. G.; Facchetti, A.; Marks, T. J. Low-temperature fabrication of high-performance metal oxide thin-film electronics via combustion processing. *Nat. Mater.* **2011**, *10*, 382–388.

[55] Zhang, H.-X.; Feng, C.; Zhai, Y.-C.; Jiang, K.-L.; Li, Q.-Q.; Fan, S.-S. Cross-stacked carbon nanotube sheets uniformly loaded with SnO_2 nanoparticles: A novel binder-free and high-capacity anode material for lithium-ion batteries. *Adv. Mater.* **2009**, *21*, 2299–2304.

[56] Vanithakumari, S. C.; Nanda, K. K. A one-step method for the growth of Ga_2O_3-nanorod-based white-light-emitting phosphors. *Adv. Mater.* **2009**, *21*, 3581–3584.

[57] Gong, S.; Schwalb, W.; Wang, Y. W.; Chen, Y.; Tang, Y.; Si, J.; Shirinzadeh, B.; Cheng, W. L. A wearable and highly sensitive pressure sensor with ultrathin gold nanowires. *Nat. Commun.* **2014**, *5*, 3132.

[58] Yaman, M.; Khudiyev, T.; Ozgur, E.; Kanik, M.; Aktas, O.; Ozgur, E. O.; Deniz, H.; Korkut, E.; Bayindir, M. Arrays of indefinitely long uniform nanowires and nanotubes. *Nat. Mater.* **2011**, *10*, 494–501.

[59] Tian, B. Z.; Liu, J.; Dvir, T.; Jin, L. H.; Tsui, J. H.; Qing, Q.; Suo, Z. G.; Langer, R.; Kohane, D. S.; Lieber, C. M. Macroporous nanowire nanoelectronic scaffolds for synthetic tissues. *Nat. Mater.* **2012**, *11*, 986–994.

[60] Weisse, J. M.; KIm, D. R.; Lee, C. H.; Zheng, X. L. Vertical transfer of uniform silicon nanowire arrays via crack formation. *Nano Lett.* **2011**, *11*, 1300–1305.

[61] Xu, F.; Liu, W.; Zhu, Y. Controlled 3D buckling of silicon nanowires for stretchable electronics. *ACS Nano* **2011**, *5*, 672–678.

[62] Jeon, D.-Y.; Pregl, S.; Park, S. J.; Baraban, L.; Cuniberti, G.; Mikolajick, T.; Weber, W. M. Scaling and graphical transport-map analysis of ambipolar schottky-barrier thin-film transistors based on a parallel array of Si nanowires. *Nano Lett.* **2015**, *15*, 4578–4584.

[63] Li, B.-R.; Hsieh, Y.-J.; Chen, Y.-X.; Chung, Y.-T.; Pan, C.-Y.; Chen, Y.-T. An ultrasensitive nanowire-transistor biosensor for detecting dopamine release from living PC12 cells under hypoxic stimulation. *J. Am. Chem. Soc.* **2013**,

135, 16034–16037.

[64] Kim, K. H.; Oh, Y.; Islam, M. F. Graphene coating makes carbon nanotube aerogels superelastic and resistant to fatigue. *Nat. Nanotechnol.* **2012**, *7*, 562–566.

[65] Shi, E. Z.; Li, H. B.; Yang, L.; Hou, J. F.; Li, Y. C.; Li, L.; Cao, A. Y.; Fang, Y. Carbon nanotube network embroidered graphene films for monolithic all-carbon electronics. *Adv. Mater.* **2015**, *27*, 682–688.

[66] Liu, Z. F.; Jiao, L. Y.; Yao, Y. G.; Xian, X. J.; Zhang, J. Aligned, ultralong single-walled carbon nanotubes: From synthesis, sorting, to electronic devices. *Adv. Mater.* **2010**, *22*, 2285–2310.

[67] Bryning, M. B.; Milkie, D. E.; Islam, M. F.; Hough, L. A.; Kikkawa, J. M.; Yodh, A. G. Carbon nanotube aerogels. *Adv. Mater.* **2007**, *19*, 661–664.

[68] Gui, X. C.; Wei, J. Q.; Wang, K. L.; Cao, A. Y.; Zhu, H. W.; Jia, Y.; Shu, Q. K.; Wu, D. H. Carbon nanotube sponges. *Adv. Mater.* **2010**, *22*, 617–621.

[69] Yang, Y. B.; Li, P. X.; Wu, S. T.; Li, X. Y.; Shi, E. Z.; Shen, Q. C.; Wu, D. H.; Xu, W. J.; Cao, A. Y.; Yuan, Q. Hierarchically designed three-dimensional macro/mesoporous carbon frameworks for advanced electrochemical capacitance storage. *Chem.—Eur. J.* **2015**, *21*, 6157–6164.

[70] Yang, Y. B.; Shi, E. Z.; Li, P. X.; Wu, D. H.; Wu, S. T.; Shang, Y. Y.; Xu, W. J.; Cao, A. Y.; Yuan, Q. A compressible mesoporous SiO_2 sponge supported by a carbon nanotube network. *Nanoscale* **2014**, *6*, 3585–3592.

[71] Kim, S. Y.; Park, S.; Park, H. W.; Park, D. H.; Jelong, Y.; Kim, D. H. Highly sensitive and multimodal all-carbon skin sensors capable of simultaneously detecting tactile and biological stimuli. *Adv. Mater.* **2015**, *27*, 4178–4185.

[72] Shin, K.-Y.; Hong, J.-Y.; Jang, J. Micropatterning of graphene sheets by inkjet printing and its wideband dipole-antenna application. *Adv. Mater.* **2011**, *23*, 2113–2118.

[73] Zhang, L. M.; Diao, S.; Nie, Y. F.; Yan, K.; Liu, N.; Dai, B. Y.; Xie, Q.; Reina, A.; Kong, J.; Liu, Z. F. Photocatalytic patterning and modification of graphene. *J. Am. Chem. Soc.* **2011**, *133*, 2706–2713.

[74] Sun, J. Y.; Gao, T.; Song, X. J.; Zhao, Y. F.; Lin, Y. W.; Wang, H. C.; Ma, D. L.; Chen, Y. B.; Xiang, W. F.; Wang, J. et al. Direct growth of high-quality graphene on high-κ dielectric $SrTiO_3$ substrates. *J. Am. Chem. Soc.* **2014**, *136*, 6574–6577.

[75] Liao, L.; Peng, H. L.; Liu, Z. F. Chemistry makes graphene beyond graphene. *J. Am. Chem. Soc.* **2014**, *136*, 12194–12200.

[76] Huang, X.; Zeng, Z. Y.; Fan, Z. X.; Liu, J. Q.; Zhang, H. Graphene-based electrodes. *Adv. Mater.* **2012**, *24*, 5979–6004.

[77] Huang, X.; Qi, X. Y.; Boey, F.; Zhang, H. Graphene-based composites. *Chem. Soc. Rev.* **2012**, *41*, 666–686.

[78] Huang, X.; Yin, Z. Y.; Wu, S. X.; Qi, X. Y.; He, Q. Y.; Zhang, Q. C.; Yan, Q. Y.; Boey, F.; Zhang, H. Graphene-based materials: Synthesis, characterization, properties, and applications. *Small* **2011**, *7*, 1876–1902.

[79] Wan, C. L.; Gu, X. K.; Dang, F.; Itoh, T.; Wang, Y. F.; Sasaki, H.; Kondo, M.; Koga, K. J.; Yabuki, K.; Snyder, G. J. et al. Flexible n-type thermoelectric materials by organic intercalation of layered transition metal dichalcogenide TiS_2. *Nat. Mater.* **2015**, *14*, 622–627.

[80] Georgious, T.; Jalil, R.; Belle, B. D.; Britnell, L.; Gorbachev, R. V.; Morozov, S. V.; Kim, Y.-J.; Gholinia, A.; Haigh, S. J.; Makarovsky, O. et al. Vertical field-effect transistor based on graphene-WS_2 heterostructures for flexible and transparent electronics. *Nat. Nanotechnol.* **2013**, *8*, 100–103.

[81] Zhang, Y.; Chang, T.-R.; Zhou, B.; Cui, Y.-T.; Yan, H.; Liu, Z. K.; Schmitt, F.; Lee, J.; Moore, R.; Chen, Y. L. et al. Direct observation of the transition from indirect to direct bandgap in atomically thin epitaxial $MoSe_2$. *Nat. Nanotechnol.* **2014**, *9*, 111–115.

[82] Baugher, B. W. H.; Churchill, H. O. H.; Yang, Y. F.; Jarillo-Herrero, P. Optoelectronic devices based on electrically tunable p-n diodes in a monolayer dichalcogenide. *Nat. Nanotechnol.* **2014**, *9*, 262–267.

[83] Kurapati, R.; Kostarelos, K.; Prato, M.; Bianco, A. Biomedical uses for 2D materials beyond graphene: Current advances and challenges ahead. *Adv. Mater.* **2016**, *28*, 6052–6074.

[84] Akinwande, D.; Petrone, N.; Hone, J. Two-dimensional flexible nanoelectronics. *Nat. Commun.* **2014**, *5*, 5678.

[85] Zhang, H. Ultrathin two-dimensional nanomaterials. *ACS Nano* **2015**, *9*, 9451–9469.

[86] Chen, Y.; Tan, C. L.; Zhang, H.; Wang, L. Z. Two-dimensional graphene analogues for biomedical applications. *Chem. Soc. Rev.* **2015**, *44*, 2681–2701.

[87] Tan, C. L.; Zhang, H. Two-dimensional transition metal dichalcogenide nanosheet-based composites. *Chem. Soc. Rev.* **2015**, *44*, 2713–2731.

[88] Huang, X.; Tan, C. L.; Yin, Z. Y.; Zhang, H. Hybrid nanostructures based on two-dimensional nanomaterials. *Adv. Mater.* **2014**, *26*, 2185–2204.

[89] Huang, X.; Zeng, Z. Y.; Zhang, H. Metal dichalcogenide nanosheets: Preparation, properties and applications. *Chem. Soc. Rev.* **2013**, *42*, 1934–1946.

[90] Wang, M.; Jang, S. K.; Jang, W.-J.; Kim, M.; Park, S.-Y.; Kim, S.-W.; Kahng, S.-J.; Choi, J.-Y.; Ruoff, R. S.; Song, Y. J. et al. A platform for large-scale graphene electronics-CVD growth of single-layer graphene on CVD-grown hexagonal boron nitride. *Adv. Mater.* **2013**, *25*, 2746–2752.

[91] Liu, S.; Lu, B.; Zhao, Q.; Li, J.; Gao, T.; Chen, Y. B.; Zhang, Y. F.; Liu, Z. F.; Fan, Z. C.; Yang, F. H. et al. Boron

nitride nanopores: Highly sensitive DNA single-molecule detectors. *Adv. Mater.* **2013**, *25*, 4549–4554.

[92] Wang, L. F.; Wu, B.; Jiang, L. L.; Chen, J. S.; Li, Y. T.; Guo, W.; Hu, P. G.; Liu, Y. Q. Growth and etching of monolayer hexagonal boron nitride. *Adv. Mater.* **2015**, *27*, 4858–4864.

[93] Sun, J.; Zheng, G. Y.; Lee, H.-W.; Liu, N.; Wang, H. T.; Yao, H. B.; Yang, W. S.; Cui, Y. Formation of stable phosphorus-carbon bond for enhanced performance in black phosphorus nanoparticle-graphite composite battery anodes. *Nano Lett.* **2014**, *14*, 4573–4580.

[94] Luo, Z.; Maassen, J.; Deng, Y. X.; Du, Y. C.; Garrelts, R. P.; Lundstrom, M. S.; Ye, P. D.; Xu, X. F. Anisotropic in-plane thermal conductivity observed in few-layer black phosphorus. *Nat. Commun.* **2015**, *6*, 8572.

[95] Yuan, J. T.; Najmaei, S.; Zhang, Z. H.; Zhang, J.; Lei, S. D.; Ajayan, P. M.; Yakobson, B. I.; Lou, J. Photoluminescence quenching and charge transfer in artificial heterostacks of monolayer transition metal dichalcogenides and few-layer black phosphorus. *ACS Nano* **2015**, *9*, 555–563.

[96] Lukatskaya, M. R.; Mashtalir, O.; Ren, C. E.; Dall'Agnese, Y.; Rozier, P.; Taberna, P. L.; Naguib, M.; Simon, P.; Barsoum, M. W.; Gogotsi, Y. Cation intercalation and high volumetric capacitance of two-dimensional titanium carbide. *Science* **2013**, *341*, 1502–1505.

[97] Liang, X.; Garsuch, A.; Nazar, L. F. Sulfur cathodes based on conductive MXene nanosheets for high-performance lithium-sulfur batteries. *Angew. Chem., Int. Ed.* **2015**, *54*, 3907–3911.

[98] Ling, Z.; Ren, C. E.; Zhao, M.-Q.; Yang, J.; Giammarco, J. M.; Qiu, J. S.; Barsoum, M. W.; Gogotsi, Y. Flexible and conductive MXene films and nanocomposites with high capacitance. *Proc. Natl. Acad. Sci. USA* **2014**, *111*, 16676–16681.

[99] Yin, H. B.; Zhu, J. P.; Guan, X. M.; Yang, Z. P.; Zhu, Y.; Zhao, H. Y.; Zhang, Z. Y.; Zhou, A. G.; Zhang, X.; Feng, C. H. et al. Effect of MXene (nano-Ti_3C_2) on early-age hydration of cement paste. *J. Nanomater.* **2015**, *2015*, Article ID 430578.

[100] Yan, W.; He, W.-Y.; Chu, Z.-D.; Liu, M. X.; Meng, L.; Dou, R.-F.; Zhang, Y. F.; Liu, Z. F.; Nie, J.-C.; He, L. Strain and curvature induced evolution of electronic band structures in twisted graphene bilayer. *Nat. Commun.* **2013**, *4*, 2159.

[101] Kuzum, D.; Takano, H.; Shim, E.; Reed, J. C.; Juul, H.; Richardson, A. G.; de Vries, J.; Bink, H.; Dichter, M. A.; Lucas, T. H. et al. Transparent and flexible low noise graphene electrodes for simultaneous electrophysiology and neuroimaging. *Nat. Commun.* **2014**, *5*, 5259.

[102] Torrisi, F.; Hasan, T.; Wu, W. P.; Sun, Z. P.; Lombardo, A.; Kulmala, T. S.; Hsieh, G.-W.; Jung, S.; Bonaccorso, F.; Paul, P. J. et al. Inkjet-printed graphene electronics. *ACS Nano* **2012**, *6*, 2992–3006.

[103] Chen, J.-H.; Ishigami, M.; Jang, C.; Hines, D. R.; Ruhrer, M. S.; Williams, E. D. Printed graphene circuits. *Adv. Mater.* **2007**, *19*, 3623–3627.

[104] Avouris, P. Graphene: Electronic and photonic properties and devices. *Nano Lett.* **2010**, *10*, 4285–4294.

[105] Weiss, N. O.; Zhou, H. L.; Liao, L.; Liu, Y.; Jiang, S.; Huang, Y.; Duan, X. F. Graphene: An emerging electronic material. *Adv. Mater.* **2012**, *24*, 5782–5825.

[106] Schwierz, F. Graphene transistors. *Nat. Nanotechnol.* **2010**, *5*, 487−496.

[107] Kim, B. J.; Jang, H.; Lee, S.-K.; Hong, B. H.; Ahn, J.-H.; Cho, J. H. High-performance flexible graphene field effect transistors with ion gel gate dielectrics. *Nano Lett.* **2010**, *10*, 3464–3466.

[108] Lee, S.-K.; Jang, H. Y.; Jang, S.; Choi, E.; Hong, B. H.; Lee, J.; Park, S.; Ahn, J.-H. All graphene-based thin film transistors on flexible plastic substrates. *Nano Lett.* **2012**, *12*, 3472–3476.

[109] Stine, R.; Robinson, J. T.; Sheehan, P. E.; Tamanaha, C. R. Real-time DNA detection using reduced graphene oxide field effect transistors. *Adv. Mater.* **2010**, *22*, 5297–5300.

[110] He, Q. Y.; Wu, S. X.; Yin, Z. Y.; Zhang, H. Graphene-based electronic sensors. *Chem. Sci.* **2012**, *3*, 1764–1772.

[111] Liu, Y. X.; Dong, X. C.; Chen, P. Biological and chemical sensors based on graphene materials. *Chem. Soc. Rev.* **2012**, *41*, 2283–2307.

[112] Mohanty, N.; Berry, V. Graphene-based single-bacterium resolution biodevice and DNA transistor: Interfacing graphene derivatives with nanoscale and microscale bio-components. *Nano Lett.* **2008**, *8*, 4469–4476.

[113] Jiang, S.; Cheng, R.; Wang, X.; Xue, T.; Liu, Y.; Nel, A.; Huang, Y.; Duan, X. F. Real-time electrical detection of nitric oxide in biological systems with sub-nanomolar sensitivity. *Nat. Commun.* **2013**, *4*, 2225.

[114] Larisika, M.; Kotlowski, C.; Steininger, C.; Mastrogiacomo, R.; Pelosi, P.; Schütz, S.; Peteu, S. F.; Kleber, C.; Reiner-Rozman, C.; Nowak, C. et al. Electronic olfactory sensor based on *A. mellifera* odorant-binding protein 14 on a reduced graphene oxide field-effect transistor. *Angew. Chem., Int. Ed.* **2015**, *54*, 13245–13248.

[115] Choi, B. G.; Park, H. S.; Park, T. J.; Yang, M. H.; Kim, J. S.; Jang, S.-Y.; Heo, N. S.; Lee, S. Y.; Kong, J.; Hong, W. H. Solution chemistry of self-assembled graphene nanohybrids for high-performance flexible biosensors. *ACS Nano* **2010**, *4*, 2910–2918.

[116] Park, S. J.; Kwon, O. S.; Lee, S. H.; Song, H. S.; Park, T. H.; Jang, J. Ultrasensitive flexible graphene based field-effect transistor (FET)-type bioelectronic nose. *Nano Lett.* **2012**, *12*, 5082–5090.

[117] An, J. H.; Park, S. J.; Kwon, O. S.; Bae, J.; Jang, J. High-performance flexible graphene aptasensor for mercury detection in mussels. *ACS Nano* **2013**, *7*, 10563–10571.

[118] Kosynkin, D. V.; Higginbotham, A. L.; Sinitskii, A.; Lomeda, J. R.; Dimiev, A.; Price, B. K.; Tour, J. M. Longitudinal unzipping of carbon nanotubes to form graphene nanoribbons. *Nature* **2009**, *458*, 872–877.

[119] Talirz, L.; Ruffieux, P.; Fasel, R. On-surface synthesis of atomically precise graphene nanoribbons. *Adv. Mater.* **2016**, *28*, 6222–6231.

[120] Bai, J. W.; Zhong, X.; Jiang, S.; Huang, Y. Duan, X. F. Graphene nanomesh. *Nat. Nanotechnol.* **2010**, *5*, 190–194.

[121] Kwon, O. S.; Park, S. J.; Hong, J.-Y.; Han, A.-R.; Lee, J. S.; Lee, J. S.; Oh, J. H.; Jang, J. Flexible FET-type VEGF aptasensor based on nitrogen-doped graphene converted from conducting polymer. *ACS Nano* **2012**, *6*, 1486–1493.

[122] Lopez-Sanchez, O.; Lambke, D.; Kayci, M.; Radenovic, A.; Kis, A. Ultrasensitive photodetectors based on monolayer MoS_2. *Nat. Nanotechnol.* **2013**, *8*, 497–501.

[123] Zhu, C. F.; Zeng, Z. Y.; Li, H.; Li, F.; Fan, C. H.; Zhang, H. Single-layer MoS_2-based nanoprobes for homogeneous detection of biomolecules. *J. Am. Chem. Soc.* **2013**, *135*, 5998–6001.

[124] He, Q. Y.; Zeng, Z. Y.; Yin, Z. Y.; Li, H.; Wu, S. X.; Huang, X.; Zhang, H. Fabrication of flexible MoS_2 thin-film transistor arrays for practical gas-sensing applications. *Small* **2012**, *8*, 2994–2999.

[125] Li, H.; Yin, Z. Y.; He, Q. Y.; Li, H.; Huang, X.; Lu, G.; Fam, D. W. H.; Tok, A. L. Y.; Zhang, Q.; Zhang, H. Fabrication of single- and multilayer MoS_2 film-based field-effect transistors for sensing NO at room temperature. *Small* **2012**, *8*, 63–67.

[126] Perkins, F. K.; Feriedman, A. L.; Cobas, E.; Campbell, P. M.; Jernigan, G. G.; Jonker, B. T. Chemical vapor sensing with monolayer MoS_2. *Nano Lett.* **2013**, *13*, 668–673.

[127] Late, D. J.; Huang, Y.-K.; Liu, B.; Acharya, J.; Shirodkar, S. N.; Luo, J. J.; Yan, A. M.; Charles, D.; Waghmare, U. V.; Dravid, V. P. et al. Sensing behavior of atomically thin-layered MoS_2 transistors. *ACS Nano* **2013**, *7*, 4879–4891.

[128] Lee, D.-W.; Lee, J.; Sohn, I. Y.; Kim, B.-Y.; Son, Y. M.; Bark, H.; Jung, J.; Choi, M.; Kim, T. H.; Lee, C. G. et al. Field-effect transistor with a chemically synthesized MoS_2 sensing channel for label-free and highly sensitive electrical detection of DNA hybridization. *Nano Res.* **2015**, *8*, 2340–2350.

[129] Chen, M. K.; Nam, H.; Rokni, H.; Wi, S. J.; Yoon, J. S.; Chen, P. Y.; Kurabayashi, K.; Lu, W.; Liang, X. G. Nanoimprint-assisted shear exfoliation (NASE) for producing multilayer MoS_2 structures as field-effect transistor channel arrays. *ACS Nano* **2015**, *9*, 8773–8785.

[130] Sarkar, D.; Liu, W.; Xie, X. J.; Anselmo, A. C.; Mitragotri, S.; Banerjee, K. MoS_2 field-effect transistor for next-generation label-free biosensors. *ACS Nano* **2014**, *8*, 3992–4003.

[131] Kim, J.; Lee, M.-S.; Jeon, S.; Kim, M.; Kim, S.; Kim, K.; Bien, F.; Hong, S. Y.; Park, J.-U. Highly transparent and stretchable field-effect transistor sensors using graphene-nanowire hybrid nanostructures. *Adv. Mater.* **2015**, *27*, 3292–3297.

[132] Myung, S.; Solanki, A.; Kim, C.; Park, J.; Kim, K. S.; Lee, K.-B. Graphene-encapsulated nanoparticle-based biosensor for the selective detection of cancer biomarkers. *Adv. Mater.* **2011**, *23*, 2221–2225.

[133] Xiao, F.; Li, Y. Q.; Zan, X. L.; Liao, K.; Xu, R.; Duan, H. W. Growth of metal-metal oxide nanostructures on freestanding graphene paper for flexible biosensors. *Adv. Funct. Mater.* **2012**, *22*, 2487–2494.

[134] Kwon, O. S.; Lee, S. H.; Park, S. J.; An, J. H.; Song, H. S.; Kim, T.; Oh, J. H.; Bae, J.; Yoon, H.; Park, T. H. et al. Large-scale graphene micropattern nano-biohybrids: High-performance transducers for FET-type flexible fluidic HIV immunoassays. *Adv. Mater.* **2013**, *25*, 4177–4185.

[135] Lee, H.; Choi, T. K.; Lee, Y. B.; Cho, H. R.; Ghaffari, R.; Wang, L.; Choi, H. J.; Chung, T. D.; Lu, N. S.; Hyeon, T. et al. A graphene-based electrochemical device with thermoresponsive microneedles for diabetes monitoring and therapy. *Nat. Nanotechnol.* **2016**, *11*, 566–572.

[136] Swisher, S. L.; Lin, M. C.; Liao, A.; Leeflang, E. J.; Khan, Y.; Pavinatto, F. J.; Mann, K.; Naujokas, A.; Young, D.; Roy, S. et al. Impedance sensing device enables early detection of pressure ulcers *in vivo*. *Nat. Commun.* **2015**, *6*, 6575.

[137] Fan, F.-R.; Lin, L.; Zhu, G.; Wu, W. Z.; Zhang, R.; Wang, Z. L. Transparent triboelectric nanogenerators and self-powered pressure sensors based on micropatterned plastic films. *Nano Lett.* **2012**, *12*, 3109–3114.

[138] Kim. S. L.; Choi, K.; Tazebay, A.; Yu, C. Flexible power fabrics made of carbon nanotubes for harvesting thermoelectricity. *ACS Nano* **2014**, *8*, 2377–2386.

[139] Yang, P.-K.; Lin, L.; Yi, F.; Li, X. H.; Pradel, K. C.; Zi, Y. L.; Wu, C.-I.; He, J.-H.; Zhang, Y.; Wang Z. L. A flexible, stretchable and shape-adaptive approach for versatile energy conversion and self-powered biomedical monitoring. *Adv. Mater.* **2015**, *27*, 3817–3824.

[140] Li, Z. T.; Wang, Z. L. Air/liquid-pressure and heartbeat-

driven flexible fiber nanogenerators as a micro/nano-power source or diagnostic sensor. *Adv. Mater.* **2011**, *23*, 84–89.

[141] Kim, T.-I.; McCall, J. G.; Jung, Y. H.; Huang, X.; Siuda, E. R.; Li, Y. H.; Song, J. Z.; Song, Y. M.; Pao, H. A.; Kim, R.-H. et al. Injectable, cellular-scale optoelectronics with applications for wireless optogenetics. *Science* **2013**, *340*, 211–217.

[142] Jeon, J.; Lee, H.-B.-R.; Bao, Z. N. Flexible wireless temperature sensors based on Ni microparticle-filled binary polymer composites. *Adv. Mater.* **2013**, *25*, 850–855.

[143] Chen, K.; Gao, W.; Emaminejad, S.; Kiriya, D.; Ota, H.; Nyein, H. Y. Y.; Takei, K.; Javey, A. Printed carbon nanotube electronics and sensor systems. *Adv. Mater.* **2016**, *28*, 4397–4414.

[144] Fukuda, K.; Takeda, Y.; Yoshimura, Y.; Shiwaku, R.; Tran, L. T.; Sekine T.; Mizukami, M.; Kumaki, D.; Tokito, S. Fully-printed high-performance organic thin-film transistors and circuitry on one-micron-thick polymer films. *Nat. Commun.* **2014**, *5*, 4147.

[145] Chen, L. Y.; Tee, B. C.-K.; Chortos, A. L.; Schwartz, G.; Tse, V.; Lipomi, D. J.; Wong, H.-S. P.; McConnell, M. V.; Bao, Z. N. Continuous wireless pressure monitoring and mapping with ultra-small passive sensors for health monitoring and critical care. *Nat. Commun.* **2014**, *5*, 5028.

[146] Shin, G. C.; Yoon, C. H.; Bae, M. Y.; Kim, Y. C.; Hong, S. K.; Rogers, J. A.; Ha, J. S. Stretchable field-effect-transistor array of suspended SnO_2 nanowires. *Small* **2011**, *7*, 1181–1185.

[147] Liu, X.; Long, Y.-Z.; Liao, L.; Duan, X. F.; Fan, Z. Y. Large-scale integration of semiconductor nanowires for high-performance flexible electronics. *ACS Nano* **2012**, *6*, 1888–1900.

[148] Wu, W. W.; Bai, S.; Yuan, M. M.; Qin, Y.; Wang, Z. L.; Jing, T. Lead zirconate titanate nanowire textile nanogenerator for wearable energy-harvesting and self-powered devices. *ACS Nano* **2012**, *6*, 6231–6235.

[149] Wei, D. C.; Liu, Y. Q. Controllable synthesis of graphene and its applications. *Adv. Mater.* **2010**, *22*, 3225–3241.

[150] Zhou, Y.; Loh, K. P. Making patterns on graphene. *Adv. Mater.* **2010**, *22*, 3615–3620.

[151] Zhu, Y.; James, D. K.; Tour, J. M. New routes to graphene, graphene oxide and their related applications. *Adv. Mater.* **2012**, *24*, 4924–4955.

[152] Hwang, S.-W.; Song, J.-K.; Huang, X.; Cheng, H. Y.; Kang, S.-K.; Kim, B. H.; Kim J.-H.; Yu, S.; Huang, Y. G.; Rogers, J. A. High-performance biodegradable/transient electronics on biodegradable polymers. *Adv. Mater.* **2014**, *26*, 3905–3911.

[153] Yin, L.; Huang, X.; Xu, H. X.; Zhang, Y. F.; Lam, J.; Cheng, J. J.; Rogers, J. A. Materials, designs, and operational characteristics for fully biodegradable primary batteries. *Adv. Mater.* **2014**, *26*, 3879–3884.

[154] Zhang, R. F.; Wen, Q.; Qian, W. Z.; Su, D. S.; Zhang, Q.; Wei, F. Superstrong ultralong carbon nanotubes for mechanical energy storage. *Adv. Mater.* **2011**, *23*, 3387–3391.

[155] Kim, S.-K.; Koo, H.-J.; Lee, A.; Braun, P. V. Selective wetting-induced micro-electrode patterning for flexible micro-supercapacitors. *Adv. Mater.* **2014**, *26*, 5108–5112.

[156] Yang, Z. B.; Deng, J.; Sun, H.; Ren, J.; Pan, S. W.; Peng, H. S. Self-powered energy fiber: Energy conversion in the sheath and storage in the core. *Adv. Mater.* **2014**, *26*, 7038–7042.

[157] Fan, F. R.; Tang, W.; Wang, Z. L. Flexible nanogenerators for energy harvesting and self-powered electronics. *Adv. Mater.* **2016**, *28*, 4283–4305.